J|A|C|S
ARTICLES
Published on Web 12/16/2003

Ruffling-Induced Chirality: Synthesis, Metalation, and Optical Resolution of Highly Nonplanar, Cyclic, Benzimidazole-Based Ligands

Tomasz Fekner, Judith Gallucci, and Michael K. Chan*

Contribution from the Department of Chemistry, The Ohio State University, 100 West 18th Avenue, Columbus, Ohio 43210

Received March 31, 2003; E-mail: chan@chemistry.ohio-state.edu

Abstract: Expedient five-step syntheses of a cyclic bis(benzimidazole)-based amide **5** and two sterically more hindered analogues **23**−**24** have been developed. These amides are chiral due to the inherent ruffling of the macrocyclic plane. Racemization of the optical antipodes of these compounds has been studied using dynamic chiral stationary phase HPLC. These studies reveal that, while the parent amide **5** racemizes rapidly, for the sterically more hindered amides **23**−**24**, the rate of racemization is significantly reduced. Bis(benzimidazole)-based amides **5** and **23**−**24** form stable Ni(II) complexes **25**−**27**, respectively. Like their parent ligands, complexes **25**−**27** are chiral due to their highly ruffled geometry. Studies of these complexes by chiral stationary phase HPLC reveal that metalation leads to a much lower rate of racemization. Incorporation of a strap can slow racemization even further. A series of strapped cyclic amides **54**−**57**, along with their corresponding dimers **58**−**61**, have been prepared. The rate of racemization for amides **54**−**57** is strongly dependent on the length of the strap. X-ray single-crystal structure analysis of the Ni(II) complex of strapped amide **54** reveals that the bis(benzimidazole) core retains its highly ruffled shape, with the two phenyl rings of the macrocycle located anti to the strap. Chiral separation of strapped ligands **54**−**57** and their corresponding Ni(II) complexes is shown to be facile by chiral stationary phase HPLC.

Introduction

Over the past decade, the study of nonplanar distortions in polyazamacrocyclic (PAM) ligands and their metal complexes has been vigorously pursued, and a remarkable plethora of out-of-plane deformation modes have been unraveled.[1,2] In particular, because protein bound porphyrinoid pigments play a key role in many vital biological systems, the main focus of attention has been on the synthesis, spectroscopy, and X-ray crystallography of porphyrins with a high degree of peripheral substitution.[3] Structural analyses of *meso*-tetraalkylporphyrins (**1**, R = H, R^1 = alkyl; Figure 1) have received particular attention, because severe quasi-equatorial interactions between the substituents R^1 attached to the *meso* carbons and the neighboring pyrrole rings lead to large nonplanar distortions.[1,2h] Studies of these synthetic porphyrins have contributed significantly to the growing awareness that nonplanar distortions have a profound effect on the biochemical, catalytic, and spectroscopic properties of porphyrins and their associated metal complexes.

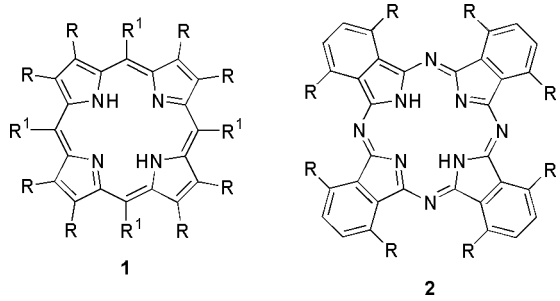

Figure 1. "Traditional" polyazamacrocyclic ligands.

Studies of other PAM systems have also been conducted to understand the effect of nonplanar distortions on their properties. For example, Kobayashi et al. have recently reported the synthesis and structural characterization of highly distorted phthalocyanines (e.g., **2**, R = Ph; Figure 1).[4] These nonplanar

(1) For a comprehensive review on the synthesis and properties of highly nonplanar porphyrins and related compounds, see: Senge, M. O. In *The Porphyrin Handbook*; Kadish, K. M., Smith, K. M., Guilard, R., Eds.; Academic Press: San Diego, 2000; Vol. 1, Chapter 6, pp 239−347.

(2) (a) Wasbotten, I. H.; Wondimagegn, T.; Ghosh, A. *J. Am. Chem. Soc.* **2002**, *124*, 8104−8116. (b) Ogura, H.; Yatsunyk, L.; Medforth, C. J.; Smith, K. M.; Barkigia, K. M.; Renner, M. W.; Melamed, D.; Walker, F. A. *J. Am. Chem. Soc.* **2001**, *123*, 6564−6578. (c) Wertsching, A. K.; Koch, A. S.; DiMagno, S. G. *J. Am. Chem. Soc.* **2001**, *123*, 3932−3939. (d) Mizuno, Y.; Aida, T.; Yamaguchi, K. *J. Am. Chem. Soc.* **2000**, *122*, 5278−5285. (e) Wondimagegn, T.; Ghosh, A. *J. Phys. Chem. A* **2000**, *104*, 4606−4608. (f) Song, X.-Z.; Jaquinod, L.; Jentzen, W.; Nurco, D. J.; Jia, S.-L.; Khoury, R. G.; Ma, J.-G.; Medforth, C. J.; Smith, K. M.; Shelnutt, J. A. *Inorg. Chem.* **1998**, *37*, 2009−2019. (g) Lin, C.-Y.; Hu, S.; Rush, T.; Spiro, T. G. *J. Am. Chem. Soc.* **1996**, *118*, 9452−9453. (h) Jentzen, W.; Simpson, M. C.; Hobbs, J. D.; Song, X.; Ema, T.; Nelson, N. Y.; Medforth, C. J.; Smith, K. M.; Veyrat, M.; Mazzanti, M.; Rammasseul, R.; Marchon, J.-C.; Takeuchi, T.; Goddard, W. A.; Shelnutt, J. A. *J. Am. Chem. Soc.* **1995**, *117*, 11085−11097. (i) Gentemann, S.; Medforth, C. J.; Forsyth, T. P.; Nurco, D. J.; Smith, K. M.; Fajer, J.; Holten, D. *J. Am. Chem. Soc.* **1994**, *116*, 7363−7368. (j) Barkigia, K. M.; Renner, M. W.; Furenlid, L. R.; Medforth, C. J.; Smith, K. M.; Fajer, J. *J. Am. Chem. Soc.* **1993**, *115*, 3627−3635. (k) Medforth, C. J.; Senge, M. O.; Smith, K. M.; Sparks, L. D.; Shelnutt, J. A. *J. Am. Chem. Soc.* **1992**, *114*, 9859−9869.

(3) For a review on nonplanar porphyrins in proteins, see: Shelnutt, J. A.; Song, X.-Z.; Ma, J.-G.; Jia, S.-L.; Jentzen, W.; Medforth, C. J. *Chem. Soc. Rev.* **1998**, *27*, 31−41.

phthalocyanines represent yet another important class of PAM ligands and their metal complexes.

One convention that has evolved as a result of the study of nonplanar PAM ligands, particularly porphyrins, is the classification of their distortions into four main modes: ruffling, saddling, doming, and waving, as proposed by Scheidt and Lee.[5] These modes serve as the basic set for the various distortions that are possible. Distortions not belonging to one particular mode can be described as a combination of the four fundamental modes.

Our interest in this arena stems from our long-standing desire to develop topologically novel chiral transition-metal complexes of PAM ligands as catalysts for asymmetric transformations. In particular, structural analysis of high-valent transition-metal oxo complexes of ruffled PAM ligands indicates that a side-on perpendicular approach of an (*E*)-alkene (or a similarly shaped substrate) to the metal center of such a complex should not encounter any significant steric obstacles.[6] As unfunctionalized prochiral (*E*)-alkenes are known to be "difficult" substrates for standard catalytic asymmetric epoxidation protocols,[7] the development of chiral, nonplanar transition-metal complexes of PAM ligands could, in principle, broaden the range and scope of existing methodologies. Recently, Gilheany et al. reported on highly enantioselective epoxidation of alkenes catalyzed by stable chromium(V)−oxo salen complexes which, in stark contrast to Jacobsen's catalytic system, provide much better enantioselectivity for (*E*)-alkenes as compared to their (*Z*)-isomers.[8,9] These results were attributed to an increased twist of the ligand backbone for the chromium salen complexes, which creates a favorable trajectory for the (*E*)-alkene to approach the chromium−oxo bond.

Because the parent porphyrin **1** (R = R[1] = H) and phthalocyanine **2** (R = H) nuclei (Figure 1) are highly symmetrical, their uniformly fully R-substituted saddled or ruffled analogues remain achiral. Cognizant of this, we focused our attention on the novel non-porphyrin bis(benzimidazole)-based ligands and their transition-metal complexes, which display a lower symmetry than the traditional PAMs (e.g., **1** and **2**) and can be rendered chiral by being locked into a ruffled conformation.[10]

Recently, we reported on the synthesis and structural characterization of the bis(benzimidazole) (BBZ) ligand **3** and a series of its transition-metal complexes **4** (M = Mn, Fe, Co, Ni, Cu) (Figure 2).[11] Although some of these compounds were demonstrated to catalyze epoxidation of styrene with promising turnover numbers (∼100), the high polarity and low solubility of ligand **3** and its complexes **4** precluded their optical resolution. In particular, we were not able to estimate the barrier to racemization for these compounds, so their stereointegrity could not be unequivocally evaluated.

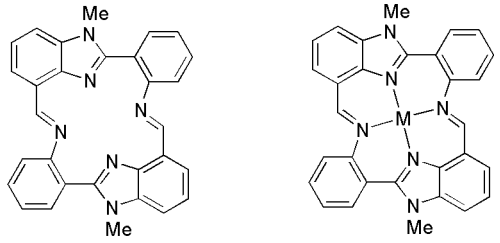

Figure 2. The original bis(benzimidazole) ligand **3** and its complexes **4**.

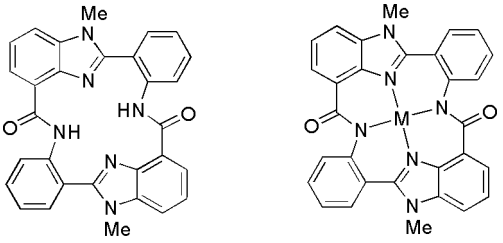

Figure 3. The amide-based bis(benzimidazole) ligand **5** and its metal complexes **6**.

As one approach toward preparing a chirally stable BBZ ligand, we decided to modify the structure of the parent BBZ macrocycle **3**.[12] The amide C−N bond is known to possess a partial double-bond character due to donation of the nonbonding electron pair on the nitrogen.[13] It was, therefore, envisaged that isosteric replacement[14] of the imine bonds in the parent BBZ ligand **3** with amide bonds (as in ligand **5**; Figure 3) would lead to macrocycles with a similar, ruffled geometry.[15] It was

(4) Kobayashi, N.; Fukuda, T.; Ueno, K.; Ogino, H. *J. Am. Chem. Soc*. **2001**, *123*, 10740−10741.
(5) Scheidt, W. R.; Lee, Y.-J. *Struct. Bonding (Berlin)* **1987**, *64*, 1−70.
(6) (a) Collman, J. P.; Zhang, X.; Lee, V. J.; Uffelman, E. S.; Brauman, J. E. *Science* **1993**, *263*, 1404−1411. (b) Groves, J. T.; Viski, P. *J. Org. Chem*. **1990**, *55*, 3628−3634. (c) Groves, J. T.; Nemo, T. E. *J. Am. Chem. Soc*. **1983**, *105*, 5786−5791.
(7) (a) Jacobsen, E. N.; Wu, M. H. In *Comprehensive Asymmetric Catalysis*; Jacobsen, E. N., Pfaltz, A., Yamamoto, H., Eds.; Springer: New York, 1999; Chapter 18.2, pp 649−677. (b) Katsuki, T. In *Catalytic Asymmetric Synthesis*, 2nd ed.; Ojima, I., Ed.; Wiley-WCH: New York, 2000; Chapter 6B.
(8) (a) O'Mahony, C. P.; McGarrigle, E. M.; Renehan, M. F.; Ryan, K. M.; Kerrigan, N. J.; Bousquet, C.; Gilheany, D. G. *Org. Lett*. **2001**, *3*, 3435−3438. (b) Daly, A. M.; Renehan, M. F.; Gilheany, D. G. *Org. Lett*. **2001**, *3*, 663−666. (c) Daly, A. M.; Dalton, C. T.; Renehan, M. F.; Gilheany, D. G. *Tetrahedron Lett*. **1999**, *40*, 3617−3620. (d) Bousquet, C.; Gilheany, D. G. *Tetrahedron Lett*. **1995**, *36*, 7739−7742.
(9) For a comprehensive overview of mechanistic aspects of transition-metal catalyzed asymmetric epoxidation of alkenes, see: Dalton, C. T.; Ryan, K. M.; Wall, V. M.; Bousquet, C.; Gilheany, D. G. *Top. Catal*. **1998**, *5*, 75−91.
(10) In porphyrins, the ruffled (*ruf*) distortion involves the alternate displacement of the *meso* carbons above and below the mean 4N-plane. By analogy, for BBZ ligands and their complexes, the *meso* carbons are those within the 16-atom inner core that are not adjacent to any of the four ligating nitrogen atoms.
(11) (a) Payra, P.; Hung, S.-C.; Kwok, W.-H.; Johnston, D.; Gallucci, J.; Chan, M. K. *Inorg. Chem*. **2001**, *40*, 4036−4039. (b) Kwok, W.-H.; Zhang, H.; Payra, P.; Duan, M.; Hung, S.-C.; Johnston, D. H.; Gallucci, J.; Skrzypczak-Jankun, E.; Chan, M. K. *Inorg. Chem*. **2000**, *39*, 2367−2376. (c) Payra, P.; Zhang, H.; Kwok, W.-H.; Duan, M.; Gallucci, J.; Chan, M. K. *Inorg. Chem*. **2000**, *39*, 1076−1080.
(12) Selected examples of amide-based ligands and complexes: (a) Moreira, R. F.; When, P. M.; Sames, D. *Angew. Chem., Int. Ed*. **2000**, *39*, 1618−1621. (b) Miller, C. G.; Gordon-Wylie, S. W.; Horwitz, C. P.; Strazisar, S. A.; Peraino, D. K.; Clark, G. R.; Weintraub, S. T.; Collins, T. J. *J. Am. Chem. Soc*. **1998**, *120*, 11540−11541. (c) Dangel, B.; Clarke, M.; Haley, J.; Sames, D.; Polt, R. *J. Am. Chem. Soc*. **1997**, *119*, 10865−10866. (d) Zhao, S.-H.; Ortiz, P. R.; Keys, B. A.; Davenport, K. G. *Tetrahedron Lett*. **1996**, *37*, 2725−2728. (e) Yoon, H.; Wagler, T. R.; O'Connor, K. J.; Burrows, C. J. *J. Am. Chem. Soc*. **1990**, *112*, 4568−4570. (f) Wagler, T. R.; Fang, Y.; Burrows, C. J. *J. Org. Chem*. **1989**, *54*, 1584−1589. (g) Kimura, E.; Shionoya, M.; Okamoto, M.; Nada, H. *J. Am. Chem. Soc*. **1988**, *110*, 3680−3682. (h) Che, C.-M.; Cheng, W.-K. *J. Chem. Soc., Chem. Commun*. **1986**, 1443−1444. (i) Kimura, E.; Koike, T.; Machida, R.; Nagai, R.; Kodama, M. *Inorg. Chem*. **1984**, *23*, 4181−4188. (j) Fabbrizzi, L.; Perotti, A.; Poggi, A. *Inorg. Chem*. **1983**, *22*, 1411−1412.
(13) Wiberg, K. B. In *The Amide Linkage*; Greenberg, A., Breneman, C. M., Liebman, J. F., Eds.; Wiley & Sons: New York, 2000; Chapter 2, pp 33−46.
(14) Patani, G. A.; LaVoie, E. J. *Chem. Rev*. **1996**, *96*, 3147−3176.
(15) A sterically restricted C−N bond seems to be a prerequisite for this class of compounds to adopt a highly ruffled geometry. This was aptly demonstrated in the case of the cyclic amine obtained by reduction of the Schiff base **3**. Single-crystal X-ray analysis revealed in this case that the two benzimidazole rings are parallel to each other, and the ruffled geometry of the parent imine **3** is not retained. Fekner, T.; Gallucci, J.; Chan, M. K., unpublished results.

Scheme 1. Retrosynthetic Analysis of Cyclic Amides **7**

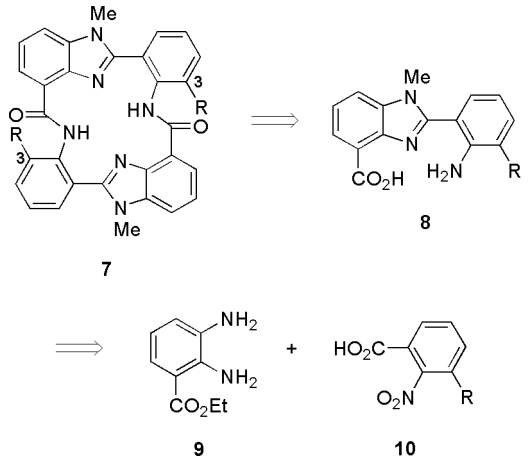

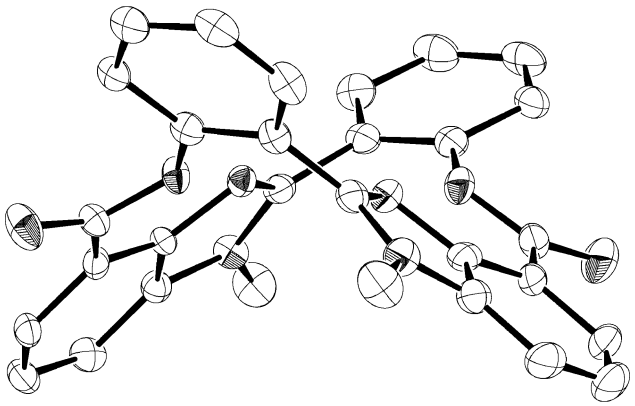

Figure 4. ORTEP drawing (50% probability thermal ellipsoids) of the molecular structure of the cyclic amide **5**. The oxygen and nitrogen atoms are hatched. Hydrogen atoms are omitted for clarity.

also expected that the cyclic amide **5** and its analogues would be more soluble in common organic solvents than the parent BBZ ligand **3**. Because diamide **5** was predicted to behave like a typical tetradentate donor, and form neutral complexes **6** with divalent cations (via metalation and concomitant loss of the amide protons), such complexes should also be more soluble in organic media. This, in turn, would be beneficial for their potential resolution by chiral stationary phase (CSP) HPLC. As the first step toward these goals, we highlight herein the synthesis, structural analysis, and metalation of ligand **5** and a series of its substituted as well as strapped analogues.

Results and Discussion

A Cyclic, Bis(benzimidazole)-Based Amide Ligand. Our first goal was the preparation of the cyclic amide **5** and its more substituted congeners. Because of the C_2 symmetry of the target molecules, their synthesis is greatly simplified. Thus, retrosynthetic cleavage (Scheme 1) of amide **7** led to amino acid **8**. Disconnecting further, amine **9**, available in multigram quantities via a five-step synthesis from commercially available 3-nitrophthalic acid,[16] and an appropriate *o*-nitrobenzoic acid **10** were selected as substrates for the preparation of the requisite amino acid **8**.

The synthesis commenced with the generation of benzimidazoles **11**−**13** (Scheme 2), which were obtained from the known diamine **9**[16] by a simple, one-pot procedure that is amenable to large-scale preparations. Thus, acylation of amine **9** with 1 equiv of an appropriate 2-nitrobenzoyl chloride in CH_2Cl_2 in the presence of Et_3N gave, in each case, a mixture of acylated products. No purification was necessary at this stage, and, after the volatiles were removed under reduced pressure, the residue was dissolved in glacial AcOH and heated to reflux in the presence of AcONa.[17] Chromatographic purification gave benzimidazoles **11**−**13** in high overall yield in each case (>90% from **9**). Deprotonation with NaH in THF, followed by chemoselective N-alkylation with MeI, gave benzimidazoles **14**−**16** as single isomers in high yield. Saponification of the ester group by boiling in 5% NaOH/MeOH furnished, after neutralization with HCl_{aq}, acids **17**−**19**, which were hydrogenated (1 atm H_2, Pd/C) to give amino acids **20**−**22**. Cyclocondensation of these amino acids under high-dilution conditions (20−23 mM in CH_2Cl_2) in the presence of the BOP Reagent/*N*-methylmorpholine (BOP/NMM)[18] gave the requisite cyclic amides **5** and **23**−**24** in moderate (46% for **5**) to excellent (78% and 86%, respectively, for **23** and **24**) yield. We attribute the increased efficiency of cyclization of amino acids **21** and **22**, relative to amino acid **20**, to the restricted rotation about the amide C−N bond for the initial monamide intermediate. Presumably, for the linear dimer (monoamide) derived from amino acids **21** and **22**, the free amino and activated carboxylic groups are forced into closer proximity, which favors intramolecular cyclodimerization over intermolecular oligomerization.

The parent cyclic amide **5** and its more sterically hindered analogues **23**−**24** are high-melting (mp > 260 °C) white powders, which in their purified forms are only sparingly soluble in common organic solvents (CH_2Cl_2, $CHCl_3$). The very low solubility of amides **23** and **24** in EtOAc, combined with their remarkably high-yielding preparation from amino acids **21** and **22**, respectively, greatly facilitates their efficient isolation from the crude reaction mixtures by simple reflux in EtOAc, followed by separation of the desired products by filtration.

Single-crystal X-ray analysis of the parent cyclic amide **5** (Figure 4) unequivocally demonstrates that, as expected from the molecular modeling studies, the molecule adopts a highly distorted, ruffled, chiral structure. The four aromatic units (benzimidazoles and *o*-substituted phenyl rings) are alternately tilted above and below the mean 4N-plane (defined by the ligating benzimidazole and amide nitrogen atoms) of the molecule. These features result in the formation of mutually perpendicular valleys above and below the macrocyclic plane and give rise to a macrocycle with two distinct diastereotopic faces. Dynamic CSP HPLC studies (Figure 5) confirm that the nonplanar, chiral geometry found in the crystalline state of amide **5** is retained in solution.

Although we were pleased to establish that the chirality of amide **5** is preserved in solution, the presence of the temperature-dependent plateau between the two peaks that correspond to the optical antipodes **5A** and **5B** indicated that interconversion of the enantiomers is fast even on the time-scale of the HPLC experiment.[19] Although the plateau-shaped CSP HPLC profiles

(16) Chapman, E.; Stephen, H. *J. Chem. Soc*. **1925**, *127*, 1791−1797.
(17) (a) Preston, P. N. In *The Chemistry of Heterocyclic Compounds*; Wiessberger, A., Taylor, E. C., Eds.; John Wiley & Sons: New York, 1981; pp 5−12. (b) Göker, H.; Ölgen, S.; Ertan, R.; Akgün, H.; Özbey, S.; Kendi, E.; Topcu, G. *J. Heterocycl. Chem*. **1995**, *32*, 1767−1773.

(18) BOP Reagent: Benzotriazol-1-yloxytris(dimethylamino)phosphonium hexafluorophosphate.

Scheme 2. Synthesis of Cyclic Amides **5**, **23**−**24**, and Their Ni(II) Complexes **25**−**27**[a]

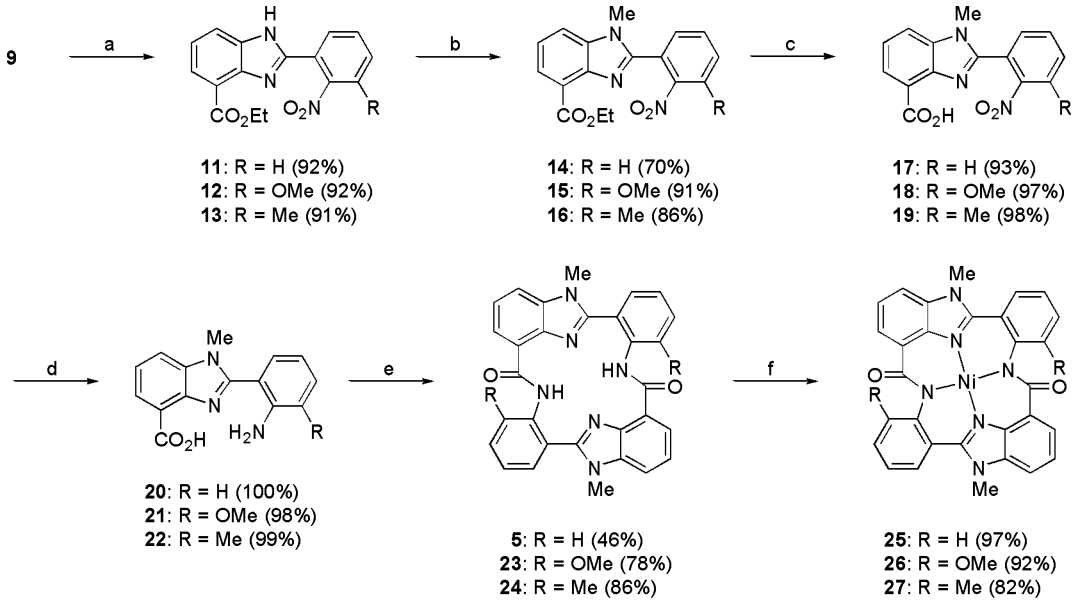

[a] Reagents and conditions: (a) 3-*R*-substituted 2-nitrobenzoyl chloride, Et_3N, CH_2Cl_2, 0 °C → room temperature, 3−6 h, then AcONa, AcOH, reflux, 15 h; (b) NaH, MeI, THF, 0 °C → room temperature, 12−13 h; (c) NaOH, MeOH, reflux, 25−50 min; (d) H_2 (1 atm), Pd/C, MeOH, room temperature, 5−24 h; (e) BOP, NMM, CH_2Cl_2, room temperature, 6−7 days; (f) $Ni(OAc)_2 \cdot 4H_2O$, MeOH, reflux, 1.5−5 h.

were not computer-simulated, comparison with the available data[19a] indicates that the half-life for racemization at room temperature for cyclic amide **5** is far less than 1000 s (an arbitrarily set threshold for feasibility of resolution of optical antipodes or other fast-interconverting entities).[20]

Because metalation was expected to increase the barrier to racemization for this class of ligands, the cyclic amide **5** (Scheme 2) was heated to reflux in MeOH in the presence of $Ni(OAc)_2$ to give a diamagnetic, bright-orange Ni(II) complex **25** in nearly quantitative yield. Complex **25** exhibits a carbonyl stretch at 1562 cm^{-1} that corresponds to a 103 cm^{-1} bathochromic shift upon concomitant deprotonation and metalation of ligand **5**.

Single-crystal X-ray analysis (Figure 6) revealed that complex **25** retains the ruffled structure of its parent ligand **5** (Figure 4) and, hence, its inherent chirality. Unlike the charged metal complexes **4** formed with the original bis(benzimidazole) ligand **3**, however, the neutral nickel complex is, as predicted, soluble in common organic solvents (especially CH_2Cl_2/MeOH mixtures). This property enabled its successful optical resolution by CSP HPLC (Figure S1).

The unusually high propensity of bis(benzimidazole) ligands and their metal complexes to accommodate high levels of nonplanar distortions is best illustrated by their comparison with two prominent representatives of other classes of PAMs.[21] The first of them is Senge's *meso*-tetrasubstituted porphyrin complex Zn(II)·H_{-2}**1**·(pyridine) (R = H, R^1 = ^{t}Bu)[22] that, like bis(benzimidazole) amide ligand **5** and complex **25**, exhibits a distinct ruffling. With an average distortion of the central 16 atoms of 0.47 Å, and a maximum displacement of its *meso* carbons by 1.01 Å, Senge's complex has been reported to be one of the most distorted porphyrins characterized to date.[23]

Similarly, Kobayashi's saddled phthalocyanine **2** (R = Ph) is the most deformed phthalocyanine (regardless of the deformation mode) reported so far.[4] For this compound, the average nonplanar distortion of its 16 central atoms is 0.22 Å, with a maximum out-of-N-plane distortion reaching 0.40 Å. In the saddle mode of distortion, it is the pyrrole carbons that exhibit the greatest nonplanar deviations. Thus, while a direct comparison of the individual distortions of phthalocyanine **2** with those for bis(benzimidazole) amide ligand **5** and its Ni(II) complex **25** is not appropriate, the absolute magnitude of their average distortions can be compared.

The distortions exhibited by cyclic amide **5** and its Ni(II) complex **25** (Figure 7) are significantly larger than the distortions observed for either Senge's porphyrin or Kobayashi's phthalocyanine. The average out-of-4N-plane distortion for the central 16 atoms of ligand **5** is 0.54 Å, that is, 0.07 Å (or 13%) higher than that for Senge's complex, and more than twice of that exhibited by Kobayashi's phthalocyanine. Similarly, the maximum distortion of 1.29 Å for the *meso* carbons in the cyclic amide **5** is considerably larger than that for Senge's porphyrin (1.01 Å). Metalation of amide **5** leads to increased ruffling of the macrocycle − the average nonplanar distortion for the central

(19) (a) Spivey, A. C.; Charbonneau, P.; Fekner, T.; Hochmuth, D. H.; Maddaford, A.; Malardier-Jugroot, C.; Redgrave, A. J.; Whitehead, M. A. *J. Org. Chem.* **2001**, *66*, 7394−7401. (b) Gasparrini, F.; Lunazzi, L.; Mazzanti, A.; Pierini, M.; Pietrusiewicz, K. M.; Villani, C. *J. Am. Chem. Soc.* **2000**, *122*, 4776−4780. (c) Spivey, A. C.; Fekner, T.; Spey, S. E.; Adams, H. *J. Org. Chem.* **1999**, *64*, 9430−9443. (d) Oxelbark, J.; Allenmark, S. *J. Org. Chem.* **1999**, *64*, 1483−1486. (e) Wolf, C.; Pirkle, W. H.; Welch, C. J.; Hochmuth, D. H.; König, W. A.; Chee, G.-L.; Charlton, J. L. *J. Org. Chem.* **1997**, *62*, 5208−5210. (f) Gasparini, F.; Lunazzi, L.; Misiti, D.; Villani, C. *Acc. Chem. Res.* **1995**, *28*, 163−170. (g) Jung, M.; Schurig, V. *J. Am. Chem. Soc.* **1992**, *114*, 529−534. (h) Veciana, J.; Crespo, M. I. *Angew. Chem., Int. Ed. Engl.* **1991**, *30*, 74−76. (i) Mannschreck, A.; Zinner, H.; Pustet, N. *Chimia* **1989**, *43*, 165−166. (j) Mannschreck, A.; Andert, D.; Eiglsperger, A.; Gmahl, E.; Buchner, H. *Chromatographia* **1988**, *25*, 182−188. (k) Eiglsperger, A.; Kastner, F.; Mannschreck, A. *J. Mol. Struct.* **1985**, *126*, 421−432. (l) Bürkle, W.; Karfunkel, H.; Schurig, V. *Chromatography* **1984**, *288*, 1−14.
(20) Oki, M. *Top. Stereochem.* **1983**, *14*, 1−81.
(21) For a compilation of data used to calculate the nonplanar distortions, see Table S21.
(22) Senge, M. O.; Ema, T.; Smith, K. M. *J. Chem. Soc., Chem. Commun.* **1995**, 733−734.
(23) For other examples of highly distorted porphyrins (*meso* carbon displacements up to 1.05 Å), see: (a) Senge, M. O.; Renner, M. W.; Kalisch, W. W.; Fajer, J. *J. Chem. Soc., Dalton Trans.* **2000**, *3*, 381−385. (b) Nelson, N. Y.; Medforth, C. J.; Nurco, D. J.; Jia, S.-L.; Shelnutt, J. A.; Smith, K. M. *Chem. Commun.* **1999**, 2071−2072.

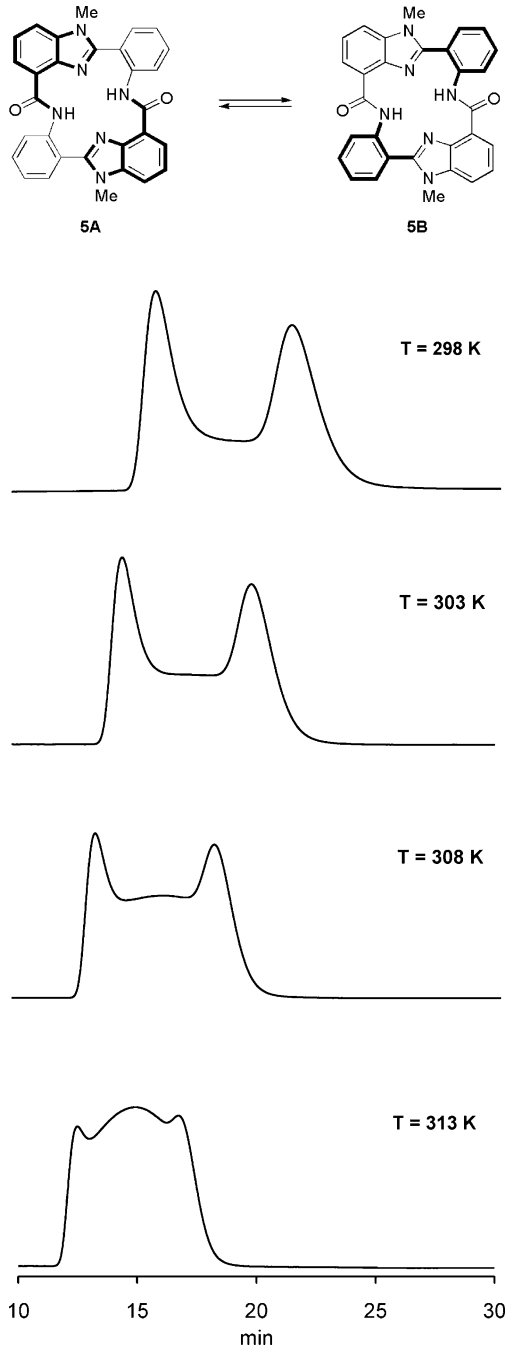

Figure 5. Macrocyclic inversion for cyclic amide **5** (4.2 μg) as determined by CSP HPLC (Chiralcel OD column, 4.6 mm × 25 cm; hexanes/2-propanol, 60/40; 1 mL min^{-1}).

atoms of ligand **5** increases from 0.54 to 0.58 Å as observed for the resulting Ni(II) complex **25**. Similarly, the average nonplanar displacement of the *meso* carbons increases from 0.94 to 1.03 Å.

The enantiomers of complex **25** (Figure S1) are significantly more stable to racemization than those of ligand **5** (Figure 5). Baseline separation of the racemic complex **25** can be achieved by CSP HPLC even at 40 °C (the upper operational limit for the column used). Nevertheless, an enantiomerically pure sample of complex **25** still racemizes at room temperature at an initial rate of ∼1% ee/day.[24] Inasmuch as direct racemization of Ni(II)-complex **25** cannot be ruled out, it is also plausible that complex **25** is in equilibrium with ligand **5**, with the latter

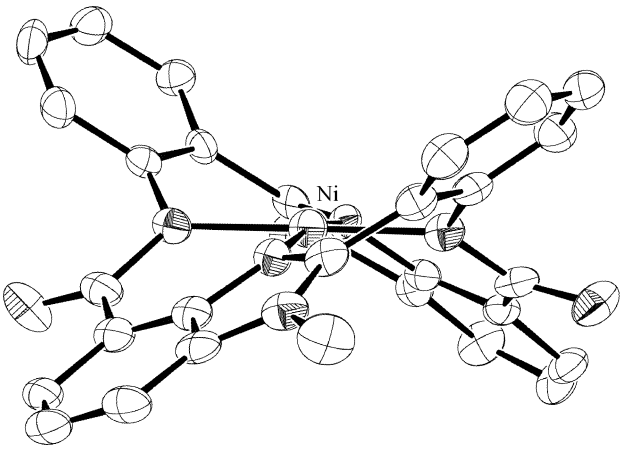

Figure 6. ORTEP drawing (50% probability thermal ellipsoids) of the molecular structure of the Ni(II) complex **25**. The nickel, oxygen, and nitrogen atoms are hatched. Hydrogen atoms are omitted for clarity.

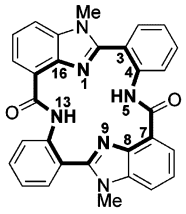

5

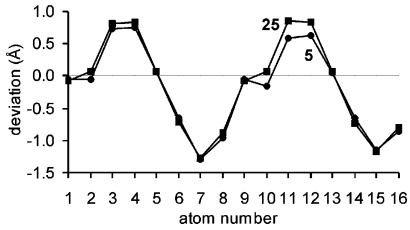

Figure 7. Deviation from planarity (Å) relative to the mean 4N-plane for the core 16 atoms in amide **5** and its Ni(II) complex **25**.

undergoing fast (see Figure 5) racemization before it re-metalates. Facile dissociation of the nickel ion from its amide-based complexes has been previously reported.[12e]

Sterically Hindered, Bis(benzimidazole)-Based Amide Ligands. A close inspection of the crystal structure of ligand **5** (Figure 4) revealed that to undergo the macrocyclic inversion (racemization), the amide carbonyl groups must move to the opposite face of the neighboring *o*-substituted phenyl rings. Thus, it seemed reasonable that increasing the steric bulk at the C-3 position of both phenyl rings (see Scheme 1 for numbering) would introduce a steric clash between these substituents and the carbonyl groups that, in turn, would hinder this racemization. Moreover, from the point of view of asymmetric catalysis, introducing a steric bulk at this position would further discriminate between the two possible trajectories, **A** and **B** (Figure 8), of the side-on approach of an (*E*)-alkene to the oxo group generated at the metal center.[25] As these trajectories require the opposite diastereotopic faces of the (*E*)-alkene to be directed toward the metal center, excluding or, at

(24) After storage in solution (2-propanol/haxanes) at room temperature for 6 days, an optically pure (ee > 99.9%) sample of complex **25** was determined to have ee = 93.6% by CSP HPLC. It can, therefore, be estimated that at room temperature ligand **5** racemizes ∼10^4 times faster than its Ni(II) complex **25**.

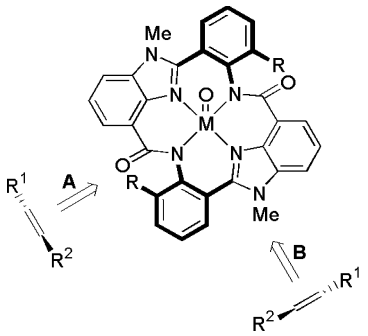

Figure 8. The two possible side-on approaches of an (*E*)-alkene toward the metal−oxo center of the ruffled complex. R^1 is sterically less demanding than R^2, and the metal−oxo bond is directed above the macrocyclic plane.

least, introducing a significant bias against one of them would result in a more efficient chirality transfer from the chiral catalyst (a ruffled metal complex) to the substrate (an alkene). The bulkier R groups would discriminate against trajectory **A**, thus ensuring a clear preference for the alternative mode of approach, **B**, which is not expected to be affected by the increased size of the R group. The above reasoning prompted us to synthesize cyclic amides **23** and **24** from amine **9** by a procedure analogous to that used for the preparation of the parent amide **5** (Scheme 2).

CSP HPLC studies revealed that, as for the parent ligand **5**, cyclic amides **23** and **24** adopt a nonplanar, chiral conformation in solution. Baseline separation of racemic cyclic amides **23** and **24** could be achieved even at 40 °C (Figures S2 and S3, respectively), demonstrating their superior stereointegrity relative to that of the parent amide **5**. Nevertheless, the barriers to macrocyclic inversion were still not sufficiently high to enable storage of optically pure samples of amides **23** and **24** for a prolonged period of time. When an enantiomerically enriched (ee = 84%) sample of amide **23** was kept in solution at room temperature for 7 h, its optical purity decreased to 42%. After an additional 11 h at room temperature, the sample was nearly racemic (ee = 13%). Because *o*-methyl groups are more efficient than *o*-methoxy groups in increasing the barrier to atropisomerization in biphenyl derivatives,[26] it was expected that a similar pattern would be observed for the barrier to macrocyclic inversion in cyclic amides **23** and **24**. Indeed, when an optically pure (ee > 99.9%) sample of cyclic amide **24** was kept in solution at room temperature for 35 h, it was determined to be of 97.1% optical purity. After 12.3 and 31.8 days at room temperature, the optical purity decreased further to 71.3% and 38.9%, respectively. When kept in boiling $CHCl_3$ (bp 61 °C), an optically pure (ee > 99.9%) sample of cyclic amide **24** was determined to have an optical purity of 23.6% after 14 h, and 5.5% after 25 h. Assuming reversible, first-order kinetics for the macrocyclic inversion, amide **23** undergoes racemization at room temperature about 90 times faster than its Me-flanked counterpart **24**.

(25) Although two diastereomeric BBZ-metal-oxo complexes are possible (with the oxo ligand either syn or anti to the phenyl rings), only one of them (with the oxo ligand syn to the phenyl rings) is considered herein. It stems from our finding (vide infra) that strapped BBZ ligands, that do not racemize as rapidly as ligands **5**, **23**, and **24**, and therefore can potentially be used in asymmetric epoxidation, have the strap located anti to the phenyl rings. As a result, only the opposite face of the macrocyclic plane is available for the oxo ligand.

(26) Eliel, E. L.; Wilen, S. H. *Stereochemistry of Organic Compounds*; J. Wiley: New York, 1994.

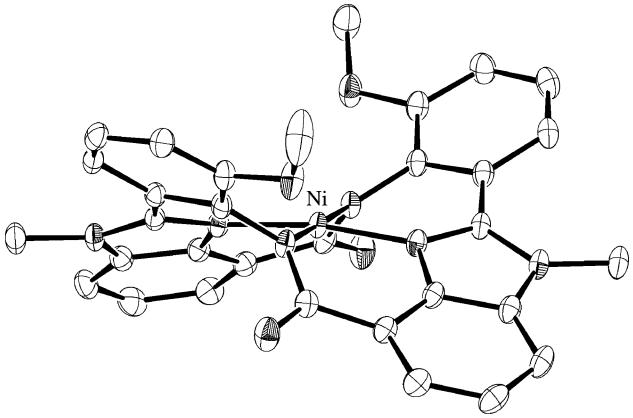

Figure 9. ORTEP drawing (50% probability thermal ellipsoids) of the molecular structure of the Ni(II) complex **26**. The nickel, oxygen, and nitrogen atoms are hatched. Hydrogen atoms are omitted for clarity.

Metalation of ligands **23** and **24** (Scheme 2) with $Ni(OAc)_2$ in MeOH furnished orange complexes **26** and **27**, respectively, in high yield. X-ray single-crystal structure analysis of complex **26** (Figure 9) confirmed that the molecule adopts a shape similar to that observed for the unsubstituted complex **25** (Figure 6). The potential steric clash between the amide carbonyls and the methoxy groups is readily apparent from the structure. Complexes **26** and **27** could be conveniently resolved by CSP HPLC (Figures S4 and S5, respectively).

Strapped, Bis(benzimidazole)-Based Amide Ligands. Faced with the problem of relatively fast racemization of ligands **5** and **23**−**24**, we decided to explore strategies that might prevent macrocyclic inversion altogether. One appealing strategy was to span the two external benzimidazole nitrogen atoms (which are not involved in metal binding) with an appropriate strap that would make racemization disallowed due to steric reasons.[27] Moreover, as in other macrocyclic cryptands,[28] such a strap could potentially be beneficial for both the thermodynamic and the kinetic stability of the complexes, as compared to their monocyclic analogues **5** and **23**−**24**. Retrosynthetic analysis (Scheme 3) indicated that the strapped ligand **28** could be prepared from amino acid **29** via double intramolecular amide bond formation. Further disconnection led to the previously prepared (see Scheme 2) benzimidazole **11** and a properly functionalized strap **30** (X − a leaving group).

In the design of these strapped ligands, the length of the strap **30** is crucial. The strap must be long enough to span the two peripheral benzimidazole nitrogen atoms in ligand **28**, but short enough to preclude ligand racemization via rotation of the core

(27) For examples of strapped and capped PAM ligands, see: (a) Bencini, A.; Bianchi, A.; Giorgi, C.; Fusi, V.; Masotti, A.; Paoletti, P. *J. Org. Chem.* **2000**, *65*, 7686−7689. (b) Wynn, T.; Hegedus, L. S. *J. Am. Chem. Soc.* **2000**, *122*, 5034−5042. (c) Hubin, T. J.; McCormick, J. M.; Collinson, S. R.; Buchalova, M.; Perkins, C. M.; Alcock, N. W.; Kahol, P. K.; Raghunathan, A.; Busch, D. H. *J. Am. Chem. Soc.* **2000**, *122*, 2512−2522. (d) Puntener, K.; Hellman, M. D.; Kuester, E.; Hegedus, L. S. *J. Org. Chem.* **2000**, *65*, 8301−8306. (e) Brandes, S.; Denat, F.; Lacour, S.; Rabiet, F.; Barbette, F.; Pallumbi, P.; Guilard, R. *Eur. J. Org. Chem.* **1998**, 2349−2360. (f) Lachkar, M.; Guilard, R.; Atmani, A.; De Cran, A.; Fissher, J.; Weiss, R. *Inorg. Chem.* **1998**, *37*, 1575−1584. (g) Brandes, S.; Lacour, S.; Denat, F.; Pallumbi, P.; Guilard, R. *J. Chem. Soc., Perkin Trans. 1* **1998**, 639−641. (h) Denat, F.; Lacour, S.; Brandes, S.; Guilard, R. *Tetrahedron Lett.* **1997**, *38*, 4417−4420. (i) Dapporto, P.; Paoli, P.; Bazzicalupi, C.; Bencini, A.; Nardi, N.; Valtoncoli, B.; Fusi, V. *Supramol. Chem.* **1996**, *7*, 195−200. (j) Springborg, J.; Olsen, C. E.; Søtofte, I. *Acta Chem. Scand.* **1995**, *49*, 555−563. (k) Weisman, G. R.; Rogers, M. E.; Wong, E. H.; Jasinski, J. P.; Paight, E. S. *J. Am. Chem. Soc.* **1990**, *112*, 8604−8605.

(28) Busch, D. H. *Chem. Rev.* **1993**, *93*, 847−860.

Scheme 3. Retrosynthetic Analysis of the Strapped Cyclic Amide **28**

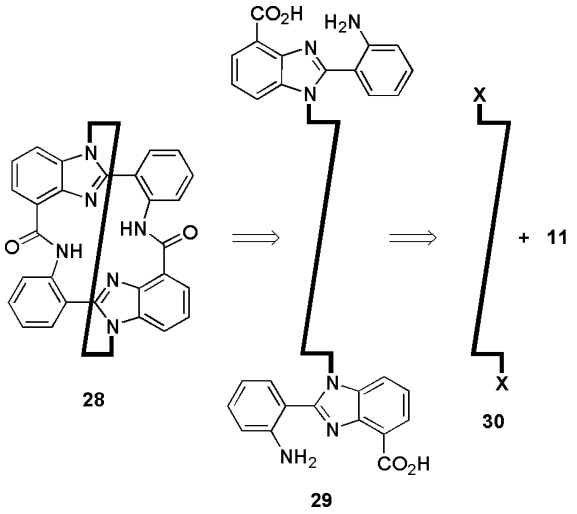

cyclic amide framework underneath the strap, or simple macrocyclic inversion without rotation (in this respect, ligand **5** can be viewed as possessing a strap of the "infinite" length). Moreover, because the strapped ligand **28** is, unlike ligand **5**, intrinsically chiral irrespective of any nonplanar distortion of the cyclic amide core, CSP HPLC would not be a suitable means to provide direct evidence for any kind of out-of-plane distortion of the cyclic amide subunit (although it remains a valuable tool in studying racemization of such ligands).

As N-alkylation of benzimidazoles with nonactivated alkyl halides is known to be difficult,[29] we opted to use benzylic bromides as the electrophiles anchoring the strap onto the benzimidazole ring. The design was convenient because the length of the strap could be adjusted by selection of an appropriate tether to join the two benzylic anchors. Thus (Scheme 4), phenol **31** was O-alkylated with a series of α,ω-dibromoalkanes in the presence of NaOH to give benzyl alcohols **33**−**36** in good yield (63−70%) and alcohol **32** in low, 29% yield. Apparently, in the case of alkylation with 1,2-dibromoethane, facile β-elimination of HBr from either the substrate or the intermediate monoether becomes a serious side reaction. When 1,2-dichloroethane was used as alkylating agent, the yield of diol **32** was even lower (7%). Upon treatment with PBr_3, alcohols **32**−**36** were converted to the corresponding benzyl bromides **37**−**41**, respectively.

With the suitable set of straps in hand, the synthesis of the geometrically restricted, strapped ligands could be undertaken. Thus, deprotonation of benzimidazole **11** (Scheme 5) with NaH in THF, followed by chemoselective alkylation with a series of benzylic bromides **38**−**41**, gave isomerically pure bis(benzimidazole)s **42**−**45**, respectively, in good to excellent yield (86−94%).[30] The $SnCl_2$-mediated reduction of the nitro groups[31] furnished amines **46**−**49**, which were then subjected to ester hydrolysis with LiOH/THF/H_2O to give, after acidic workup,

Scheme 4. Synthesis of Benzylic Bromides **37**−**41**[a]

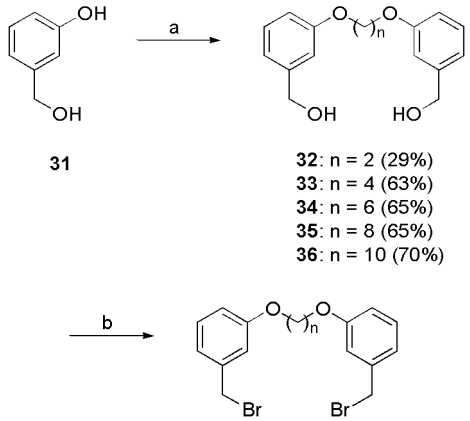

[a] Reagents and conditions: (a) 1,*n*-dibromoalkane (n = 2, 4, 6, 8, 10), NaOH, EtOH, H_2O reflux, 10−48 h; (b) PBr_3, CH_2Cl_2, 0 °C → room temperature, 11−16 h.

amino acids **50**−**53** in good overall yield (87−90% over two steps). High-dilution (4.2−9.4 mM in CH_2Cl_2) cyclocondensation of amino acids **50**−**53** in the presence of BOP/NMM gave strapped monomers **54**−**57** and their corresponding dimers **58**−**61** in low yield. Although pure samples of the monomers are slightly soluble in CH_2Cl_2 and $CHCl_3$ (but not EtOAc), the solubility of analytically pure samples of the dimers in all of these solvents is low. Additionally, as dimers **58** and **59** exhibit a lower solubility than dimers **60** and **61** (a property that made recording of NMR spectra of dimer **58** prohibitively difficult), dimer solubility appears to be a function of the distance between the two bis(benzimidazole) rings. Despite their poor solubility, chromatographic purification (see Experimental Section) of the crude mixtures from the cyclocondensation reaction of amino acids **50**−**53** was never plagued by crystallization of the products on the column.

Upon treatment with $Ni(OAc)_2$ in boiling MeOH, the strapped ligand **54** gave a deep-orange Ni(II) complex **62** in nearly quantitative yield (Scheme 6). As seen for a series of the nonstrapped ligands **5** and **23**−**24** and their Ni(II)-complexes **25**−**27**, metalation leads to a bathochromic shift for the amide carbonyl stretching by 102 cm^{-1} (from 1678 to 1576 cm^{-1}) for the strapped Ni(II)-complex **62** as compared to the free ligand **54**. Single-crystal X-ray diffraction analysis of complex **62** (Figure 10) confirmed that the core cyclic amide adopts a ruffled conformation, and its geometry appears to be controlled by the position of the strap (vide infra, for discussion).

^1H NMR analysis of the series of monomers **54**−**57** revealed that significant differences in chemical shifts could be observed only for the aromatic proton H_a and two pairs of diastereotopic protons $H_b/H_{b'}$ and $H_c/H_{c'}$ (Table 1). Molecular modeling based on the X-ray single-crystal structure of the Ni(II) complex **62** (Figure 10) indicates that these protons are located directly above the 10-electron aromatic benzimidazoles and, thus, are within the shielding cone of the aromatic ring current.[32] Because the intensity of the anisotropic field diminishes rapidly with distance, the corresponding protons in the monomers possessing shorter straps would be expected to experience a more pronounced

(29) Muller, G.; Bünzil, J.-C. G.; Schenk, K. J.; Piguet, C.; Hopfgartner, G. *Inorg. Chem.* **2001**, *40*, 2642−2651.
(30) Analytically pure samples of benzimidazoles **42**−**45** exhibit liquid-crystal-like properties. When heated, they initially turn into hazy liquids (mp 170 °C for **42**, 172 °C for **43**, 82 °C for **44**, and 100 °C for **45**). The clearing temperature (transition from mesophase to isotropic liquid) is significantly higher (180 °C for **42**, 186 °C for **43**, 93 °C for **44**, and 118 °C for **45**). The highly polar nitro groups located at each end of these elongated molecules are most likely responsible for this phenomenon.
(31) Bellamy, F. D.; Ou, K. *Tetrahedron Lett.* **1984**, *25*, 839−842.

Scheme 5. Synthesis of Strapped Cyclic Amides **54**−**57** and Dimers **58**−**61**[a]

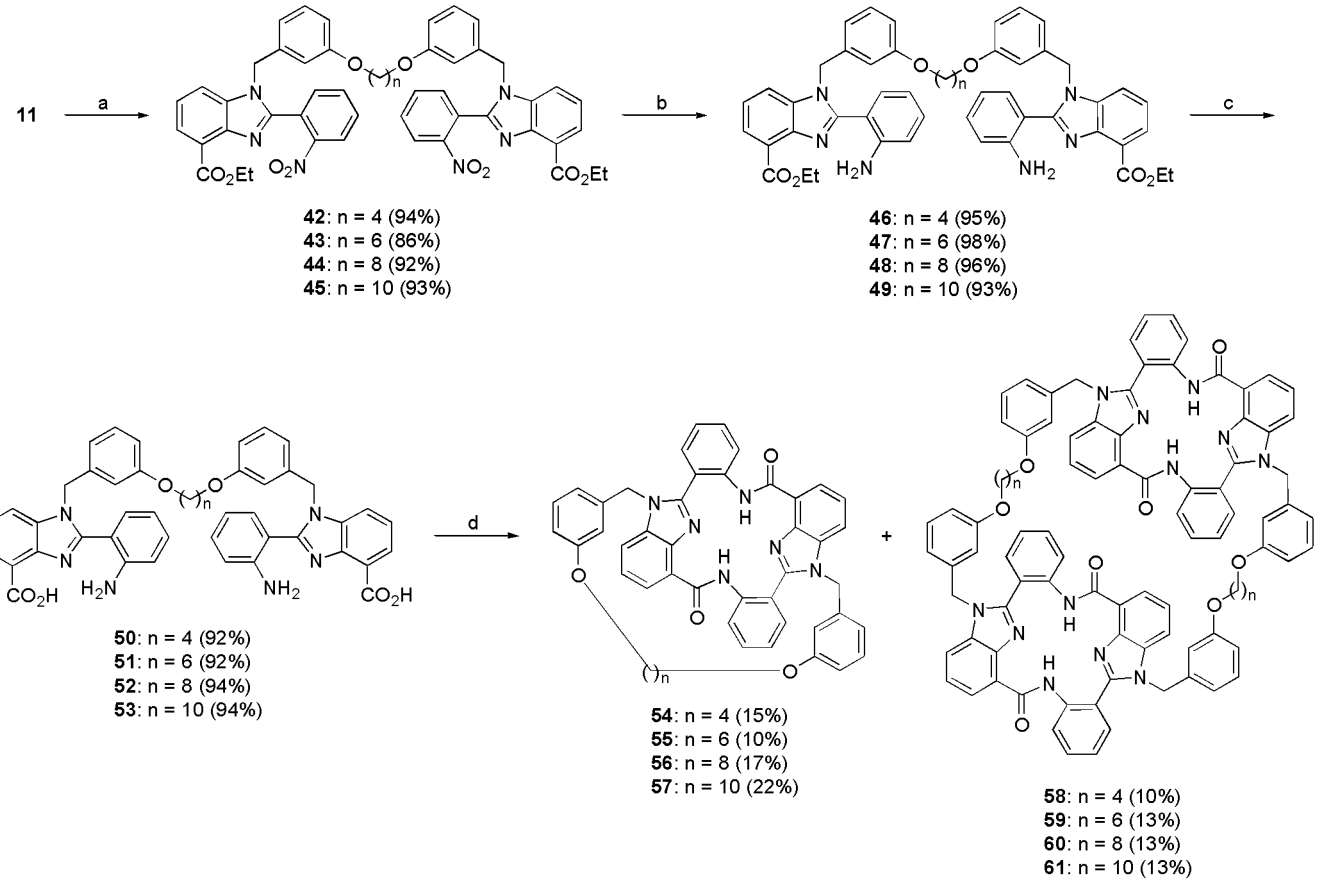

[a] Reagents and conditions: (a) NaH, **38**−**41**, THF, 0 °C → room temperature, 14−20 h; (b) $SnCl_2$, EtOH, reflux, 45−50 min; (c) LiOH, THF, H_2O, room temperature, 15−20 h; (d) BOP, NMM, CH_2Cl_2, room temperature, 7−10 days.

Scheme 6. Metalation of the Strapped Cyclic Amide **54**[a]

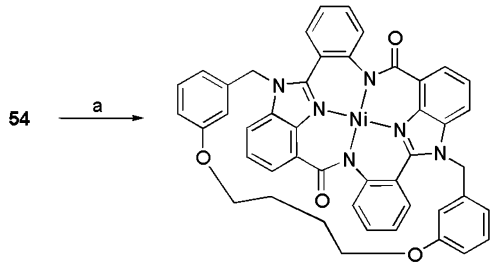

[a] Reagents and conditions: (a) $Ni(OAc)_2 \cdot 4H_2O$, MeOH, reflux, 2 h; 94%.

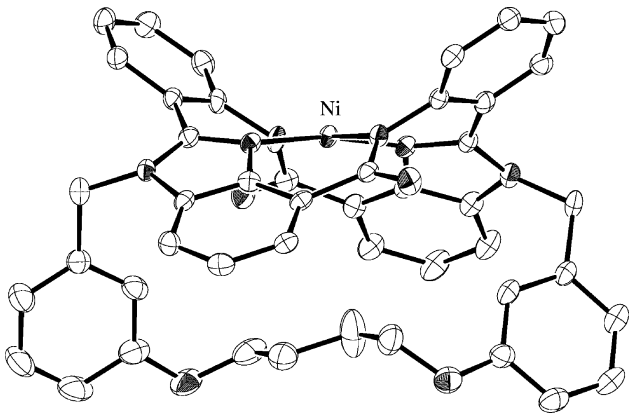

Figure 10. ORTEP drawing (50% probability thermal ellipsoids) of the molecular structure of the Ni(II) complex **62**. The nickel, oxygen, and nitrogen atoms are hatched. Hydrogen atoms are omitted for clarity.

upfield shift due to the geometric constraints that force their close spatial proximity with the aromatic system. As illustrated in Table 1, this is found to be the case.

The length of the strap in compounds **54**−**57** not only affects their NMR spectra but also, and more importantly, is directly related to the ability of the strap to hinder racemization. Because for the strapped amides **54**−**57** we did not observe any evidence, either spectroscopic (^1H and ^{13}C NMR) or chromatographic (CSP HPLC), that these compounds exist as mixtures of more than one diastereomer, it appears that the act of racemization for this class of compounds must involve concerted rotation of the core cyclic amide under the strap (which results in inversion of configuration at the two stereogenic benzimidazole nitrogen atoms) accompanied by its macrocyclic inversion. Consistent with molecular modeling studies, the X-ray single-crystal structure of the Ni(II) complex **62** (Figure 10) of the strapped cyclic amide **54** indicates that the geometry of the core cyclic bis(benzimidazole) part of the molecule is governed by the position of the strap, with the two benzimidazoles pointing toward it, and the two *o*-substituted phenyl rings occupying the opposite face of the 4N-plane. This preference stems from the intrinsic puckering of the cyclic amide core (cf., Figures 4, 6,

(32) (a) Waugh, J. S.; Fessenden, R. W. *J. Am. Chem. Soc.* **1957**, *79*, 846−849. (b) Pople, J. A.; Schneider, W. G.; Bernstein, H. J. *High-Resolution Nuclear Magnetic Resonance*; McGraw-Hill: New York, 1959. (c) Günther, H. *NMR Spectroscopy*; Wiley: New York, 1998. (d) Gomes, J. A. N. F.; Mallion, R. B. *Chem. Rev.* **2001**, *101*, 1349−1384.

Scheme 7. Cyclization Studies of Amino Acids **63**−**65**[a]

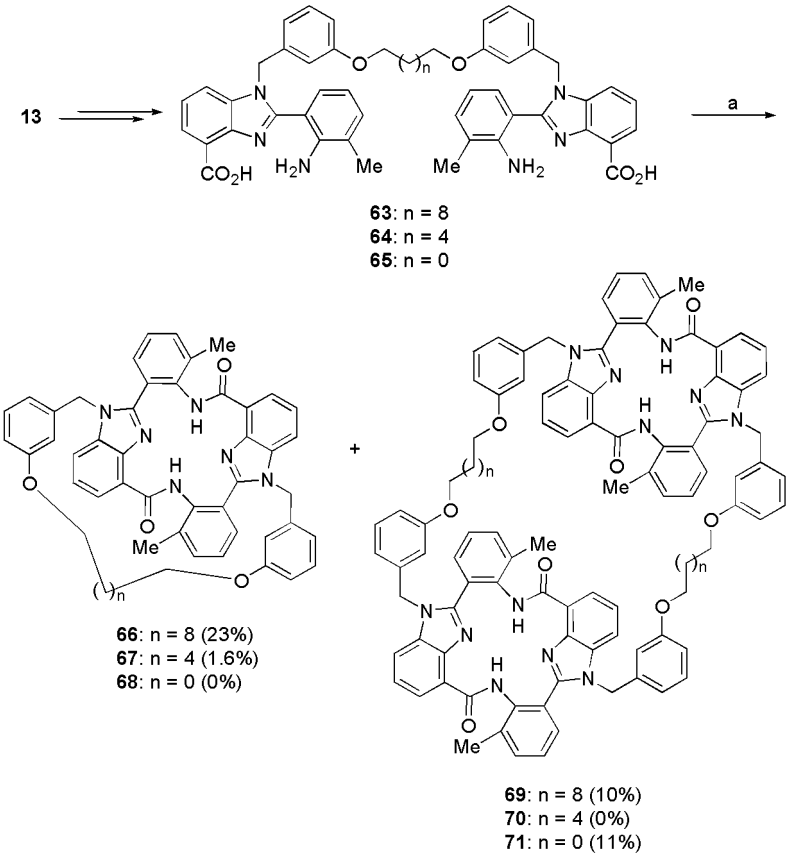

[a] Reagents and conditions: (a) BOP, NMM, CH_2Cl_2, room temperature, 7−9 days.

Table 1. Selected ^{1}H NMR Signals for Strapped Cyclic Amides **54**−**57**[a]

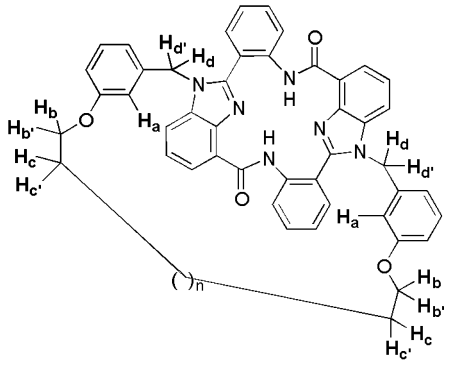

54-57 (n = 0, 2, 4, 6)

	δ/ppm[b]			
	H_a (s)	$H_b/H_{b'}$ (m)	$H_c/H_{c'}$ (m)	$H_d/H_{d'}$ (ABq)
54	5.22	2.90−3.05	0.00−0.12 0.22−0.33	5.38/5.77
55	5.71	3.41 (t)	0.57−0.68	5.30/5.78
56	6.17	3.51−3.59 3.68−3.75	1.26−1.44	5.26/5.78
57	6.43	3.62−3.70 3.78−3.85	1.50−1.66	5.18/5.72

[a] Spectra were recorded in $CDCl_3$ (400 MHz) and referenced to the residual $CHCl_3$ peak. [b] The $H_c/H_{c'}$ signals were correlated to the $H_b/H_{b'}$ signals via ^{1}H−^{1}H 2D COSY spectroscopy.

and 9), for which substituents attached to the external benzimidazole nitrogen atoms are situated on the same face of the mean 4N-plane as the benzimidazole phenyl rings. As a result, at least for relatively short straps, the macrocyclic core is forced to adopt the conformation for which the distance to be spanned by the strap is the shortest (the same face as the benzimidazole phenyl rings), and, consequently, the strain introduced is minimized. For longer straps, however, the macrocyclic inversion is expected to be relatively free (as it is for amide **5**) and independent from any rotation of the macrocyclic core under the strap.

As cyclodimerization of sterically hindered amino acids **21** and **22** was more efficient than that of the parent amino acid **20** (Scheme 2), we also investigated whether the presence of the bulkier flanking substituent was beneficial for the cyclization of tethered bis(amino acid)s, as well. Thus (Scheme 7), benzimidazole **13** was converted to amino acids **63**−**65** (Scheme S1) by a synthetic route analogous to that described for the preparation of amino acids **50**−**53** from benzimidazole **11** (Scheme 5). Cyclization of amino acid **63** under standard conditions gave monomer **66** in 23% yield, along with dimer **69** in 10% yield. These yields are comparable to those obtained for the cyclization of the "H-flanked" amino acid **55** (Scheme 5; monomer, 22%; dimer, 13%). Amino acid **64** proved a very poor substrate for cyclization under the standard conditions due to its extremely low solubility in CH_2Cl_2. Only a small amount (1.6%) of monomer **67** was isolated in this case after a prolonged reaction time (9 days). When subjected to the cyclization protocol, amino acid **65**, possessing an extremely short strap, gave dimer **71** in 11% yield. The corresponding monomer was not isolated, presumably because its formation is thermody-

Table 2. Racemization of Strapped Cyclic Amides **54**−**56** and **66**[a,b]

	room temp (~25 °C)[c]		$CHCl_3$ (bp 61 °C)		PhH (bp 80 °C)		PhMe (bp 111 °C)	
compound	time/h	ee/%	time/h	ee/%	time/h	ee/%	time/h	ee/%
54	0	99.4					0	>99.9
	404	99.4					14.6	>99.9
	1751	99.4					304	>99.9
55	0	99.5			0	>99.9		
	529	99.5			74	96.5		
	1873	99.5			217	88.7		
56	0	99.7	0	>99.9				
	255	99.7	143	97.5				
	716	99.7	255	95.2				
	2011	99.7						
66	0	>99.9	0	99.7	0	>99.9		
	47	99.3	3.5	92.3	25	0		
	234	97.3	18.7	67.2				
	645	93.0	43.4	39.4				
	1964	80.0						

[a] Racemization was performed in the indicated solvents at their boiling-point temperatures. [b] Enantiomeric excess (ee) was determined by analytical CSP HPLC. [c] Samples were kept in $CHCl_3$ at ambient temperature.

namically disfavored due to the high strain energy associated with spanning the bis(benzimidazole) diamide with such a short strap.

To evaluate the effect of the strap length on the rate of racemization for the series of monomeric strapped amides, ligands **54**−**56** were optically resolved using CSP HPLC, and the optical purity of the ligands was measured after a given racemization period. As we were not able to satisfactorily resolve compound **57** on a wide range of CSP HPLC columns available to us, compound **66** (Scheme 7), which possesses the identical strap and proved amenable to optical resolution, was vicariously used in the racemization studies. These studies were performed at various temperatures, ranging from ~25 °C (room temperature) to 111 °C (bp of PhMe), and their results are summarized in Table 2. As can be noted, only compound **66**, possessing the longest strap, undergoes racemization at room temperature to any significant degree, losing 0.7% ee after 47 h, and 20% ee after ~82 days. The stereointegrity of the compounds possessing shorter straps is sufficiently high to prevent racemization at room temperature, although monomers **55** and **56** do racemize at elevated temperatures.

In a related fashion, dimers **58**−**61** can be thought of as monomers with extremely long straps. As such, one ruffled cyclic amide can be considered a part of a long strap spanning the two external benzimidazole nitrogen atoms of the other ruffled cyclic amide. Molecular modeling studies indicate that for dimers **58**−**61** the two cyclic amides are held strictly in a face-to-face orientation. In terms of stereochemistry, however, this type of dimerization for the ruffled C_2-symmetric molecules is potentially considerably more complex than the simple spanning discussed previously for monomers **54**−**57**. As mentioned previously for the cyclic amide monomers with extremely long straps, macrocyclic inversion of the individual monomers forming the dimer should be possible without the need for rotation of the macrocycle under the strap. Moreover, as the two cyclic amides of dimers **58**−**61** can face each other in three different fashions (*R*-*R*/*R*-*R*, *R*-*R*/*S*-*S*, and *S*-*S*/*S*-*S*; depending on the configuration generated at the two pairs of the stereogenic benzimidazole nitrogens), the dimers can potentially exist as mixtures of four pairs of enantiomers (**rac 1**−**4**) and two achiral forms (**meso 1**,**2**) (Figure 11), with each compound being at least C_2-symmetric.[33] Any of the 10 possible isomers can be formally converted into any other by macrocyclic inversion of either cyclic amide, rotation of one macrocycle under the "strap", or a combination of these two basic transformations.

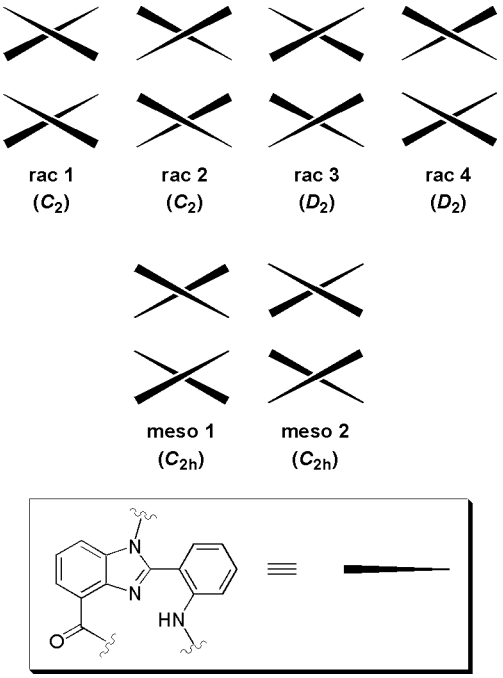

Figure 11. The set of possible stereoisomers from dimerization of a C_2-symmetric, ruffled molecule.

The barrier to rotation under the strap depends on the distance between the two cyclic amides, whereas the barrier to macrocyclic inversion is a function of steric constraints within the cyclic amide core (vide supra). Spectroscopic data (^{1}H and ^{13}C NMR) indicate that the medium-length strap dimers **59**−**60** exist, at least on the NMR time-scale, either as nearly equimolar mixtures of two diastereomers with either D_2 or C_{2h} symmetry (Figure 11) or as diastereomerically homogeneous samples of C_2-symmetric molecules. For instance, the ^{1}H NMR (400 MHz, $CDCl_3$) spectrum of dimer **60** shows two singlets (12.01 and 12.02 ppm) for the amide protons, as well as two singlets (6.34 and 6.37 ppm) for the H_a (see Table 1 for labeling system), with many other peaks broadened or showing unusual multiplicities. The proton-decoupled ^{13}C NMR (101 MHz, $CDCl_3$) spectrum of dimer **60** consists of 32 signals, whereas only 25 signals would be expected for a diastereomerically homogeneous sample of either D_2- or C_{2h}-symmetric molecules. If dimers **59** and **60** are diastereomerically pure, they most likely exist as **rac 1** (Figure 11) for which the π-stacking interaction between the two cyclic amide subunits is maximized.

Although CSP HPLC studies of dimers **58**−**61** were not very successful due to their high affinity toward the CSPs used, it was possible to partially resolve the related dimer **69** formed from the dimethyl-substituted macrocycle. In this case, the HPLC trace (Figure S11) shows the presence of five peaks,

(33) For the sake of simplicity, the side-on view (as in Figure 4) of the ruffled cyclic amide is represented in Figure 11 by two crossed wedged lines, with their sharp ends representing the *o*-substituted phenyl rings, and their wide ends representing the benzimidazole parts of the molecule. The straps have been omitted for clarity.

which could be attributed to two racemates and one *meso* form. NMR studies performed on the related short-length strap dimer **71** reveal it to have much simpler ^{1}H and ^{13}C NMR spectra than the medium-length strap dimers **59** and **60**. Based on its NMR, the two cyclic amide subunits of **71** appear to be in chemically equivalent environments. Symmetry considerations (Figure 11) indicate that at room temperature molecules of dimer **71** in the most thermodynamically stable geometry belong to either point group D_2 (**rac 3**, **rac 4**) or point group C_{2h} (**meso 1**, **meso 2**). Apparently, the very short distance between the two cyclic bis(benzimidazole) subunits fixes the macrocycle in a well-defined conformation for which neither macrocyclic inversion nor rotation of the cyclic amide under the strap can take place. These symmetry considerations would rule out the "ideal" π-stacking between the two cyclic amide subunits (as in C_2-symmetric **rac 1**), although the inverted π-stacking interactions of the phenyl and benzimidazole units as observed for **rac 3** and **rac 4** are still possible.

Conclusions

In summary, we have developed a practical synthesis of cyclic bis(benzimidazole)-based amides **5** and **23**−**24**. These ligands were demonstrated to possess a highly distorted, ruffled, chiral structure. Because of the greater solubility of these compounds as compared to ligand **3**, their optical resolution and racemization could be studied by CSP HPLC. While the incorporation of steric hindrance into amides **23**−**24** lowered the rate of racemization, the effect was not sufficient to enable storage of enantioenriched samples for a prolonged period of time without significant loss of optical purity. Metalation with Ni(II) was also demonstrated to increase the barrier to macrocyclic inversion for this class of compounds. The problem of macrocyclic inversion could be completely circumvented by spanning the two external benzimidazole nitrogen atoms of the parent bis(benzimidazole) framework with the tailor-made straps of various lengths. These compounds and their corresponding Ni(II) complexes were amenable to optical resolution by CSP HPLC and were demonstrated to be chirally stable at ambient temperature. Work is currently underway to prepare other ligands of this class and their complexes with various transition metals as potential catalysts for asymmetric transformations.

Experimental Section

General Methods. All reactions were performed under anhydrous conditions and in an inert atmosphere of argon using oven-dried glassware. Yields refer to chromatographically and spectroscopically (^{1}H NMR) homogeneous materials, unless otherwise indicated. Reagents were used as obtained from commercial sources or purified according to known procedures.[34] Flash chromatography was carried out using Merck Kiesegel 60 F_{254} (230−400 mesh) silica gel following the method of Still et al.[35] Only distilled solvents were used as eluents. Thin-layer chromatography (TLC) was performed on Merck DC-Alufolien or glass plates precoated with silica gel 60 F_{254} which were visualized either by quenching of ultraviolet fluorescence or by charring with 5% w/v phosphomolybdic acid in 95% EtOH, 10% w/v ammonium molybdate in 1 M H_2SO_4, or 10% $KMnO_4$ in 1 M H_2SO_4. Observed retention factors (R_f) are quoted to the nearest 0.05. All reaction solvents were distilled before use and stored over activated 4 Å molecular sieves, unless otherwise indicated. Anhydrous CH_2Cl_2 was obtained by refluxing over CaH_2. Anhydrous THF was obtained by distillation, immediately before use, from sodium/benzophenone ketyl under an inert atmosphere of nitrogen. Petroleum ether refers to the fraction of light petroleum boiling between 40 and 60 °C. High-resolution mass spectrometry (HRMS) measurements are valid to ±5 ppm. Melting points (mp) are quoted to the nearest 0.5 °C. Elemental analyses were performed by Atlantic Microlab, Norcross, GA.

Ethyl 2-(2-Nitrophenyl)-1*H*-benzimidazole-4-carboxylate (11). To a solution of oxalyl chloride (22.7 mL, 0.26 mol) in CH_2Cl_2 (250 mL) were added 2-nitrobenzoic acid (33.4 g, 0.20 mol) and a catalytic amount of DMF (∼2 drops). The reaction mixture was stirred at room temperature for 12 h to give a clear solution. The volatiles were removed in vacuo to afford the crude acyl chloride product as a pale brown oil (37.2 g). A solution of the acyl chloride in CH_2Cl_2 (400 mL) was added dropwise over 2 h at 0 °C to a solution of diamine **9** (34.9 g, 194 mmol) and Et_3N (36 mL, 0.26 mol) in CH_2Cl_2 (1600 mL). After the addition was complete, the reaction mixture was stirred at 0 °C for 1 h and at room temperature for 3 h. The volatiles were removed in vacuo to give an off-white solid. Analysis of the crude product [^{1}H NMR (250 MHz, $CDCl_3$)] revealed the presence of two isomeric monamides in a ca. 5:1 ratio. The crude amide mixture was refluxed in glacial AcOH (500 mL) in the presence of AcONa (16.4 g, 0.20 mol) for 15 h. The reaction mixture was cooled to room temperature and evaporated in vacuo. The resulting brown oil was partitioned between CH_2Cl_2 and water. After neutralization with solid K_2CO_3, the phases were separated, and the extraction was completed with additional portions of CH_2Cl_2. The combined organic extracts were dried ($MgSO_4$) and evaporated in vacuo to give a brown solid. Purification by flash chromatography (silica gel, CH_2Cl_2 → EtOAc) gave the title compound **11** (56.1 g, 93% over two steps from diamine **9**) as a bright yellow solid: $R_f = 0.70$ (EtOAc/CH_2Cl_2, 1/1); mp 115.0−116.0 °C (EtOAc/petroleum ether). ^{1}H NMR (250 MHz, $CDCl_3$): δ 1.26 (t, $J = 7.0$ Hz, 3H), 4.23 (q, $J = 7.0$ Hz, 2H), 7.17 (t, $J = 8.0$ Hz, 1H), 7.36−7.49 (m, 2H), 7.73−7.84 (m, 4H), and 11.0 (br s, 1H). ^{13}C{^{1}H} NMR (63 MHz, $CDCl_3$): δ 14.72, 61.70, 114.6, 122.5, 125.0, 125.2, 125.6, 126.0, 131.2, 132.5, 133.2, 135.0, 144.6, 148.9, 149.1, and 166.6. IR ($CHCl_3$): υ_{max} 1694, 1534, 1371, 1280, 1196, and 1145 cm^{-1}. MS (ESI): *m*/*z* (rel intensity) 312 (30%, MH^+), 284 (100), and 266 (40). HRMS calcd for $C_{16}H_{13}N_3NaO_4$ (MNa^+) 334.0804, found 334.0807. Anal. Calcd for $C_{16}H_{13}N_3O_4$: C, 61.73; H, 4.21; N, 13.50. Found: C, 61.89; H, 4.13; N, 13.43.

Ethyl 1-Methyl-2-(2-nitrophenyl)-1*H*-benzimidazole-4-carboxylate (14). To a solution of benzimidazole **11** (55.3 g, 178 mmol) in THF (500 mL) was slowly added NaH (60% w/w dispersion in mineral oil, 7.82 g, 0.20 mol) at 0 °C. After 30 min, the reaction mixture was warmed to room temperature and stirred for an additional 40 min. The resulting brown solution was recooled to 0 °C and quenched with MeI (28 mL, 0.45 mol). After 13 h at room temperature, the volatiles were removed in vacuo, and the residue was partitioned between CH_2Cl_2 and water. The phases were separated, and the extraction was completed with additional portions of CH_2Cl_2. The combined organic extracts were dried ($MgSO_4$) and evaporated in vacuo to give a yellow solid. Purification by flash chromatography (silica gel, CH_2Cl_2 → EtOAc) gave the title compound **14** (53.2 g, 92%) as a pale yellow solid: $R_f = 0.40$ (EtOAc/CH_2Cl_2, 1/1); mp 163.0−164.0 °C (EtOAc/petroleum ether). ^{1}H NMR (250 MHz, $CDCl_3$): δ 1.26 (t, $J = 7.0$ Hz, 3H), 3.46 (s, 3H), 4.31 (q, $J = 7.0$ Hz, 2H), 7.22 (t, $J = 8.0$ Hz, 1H), 7.43 (dd, $J = 8.0$, 1.0 Hz, 1H), 7.51−7.64 (m, 3H), 7.82 (dd, $J = 7.5$, 1.0 Hz, 1H), and 8.04−8.07 (m, 1H). ^{13}C{^{1}H} NMR (63 MHz, $CDCl_3$): δ 14.81, 31.17, 61.23, 114.4, 122.4, 122.7, 125.2, 125.4, 126.4, 131.6, 133.6, 134.0, 137.2, 142.5, 149.0, 152.0, and 166.1. IR ($CHCl_3$): υ_{max} 1715, 1535, 1460, 1347, 1281, 1251, and 1124 cm^{-1}. MS (ESI): *m*/*z* (rel intensity) 348 (5%, MNa^+), 326 (55, MH^+), and 298 (100). HRMS calcd for $C_{17}H_{15}N_3NaO_4$ (MNa^+) 348.0960, found 348.0973. Anal. Calcd for $C_{17}H_{15}N_3O_4$: C, 62.76; H, 4.65; N, 12.92. Found: C, 62.77; H, 4.65; N, 12.91.

(34) Perrin, D. D.; Armarego, W. L. F. *Purification of Laboratory Chemicals*; Pergamon Press: New York, 1988.
(35) Still, W. C.; Hahn, M.; Mitra, A. *J. Org. Chem.* **1978**, *43*, 2923−2925.

1-Methyl-2-(2-nitrophenyl)-1*H*-benzimidazole-4-carboxylic Acid (17). To a solution of NaOH (10.0 g, 0.40 mol) in MeOH (250 mL) was added ester **14** (19.7 g, 60.6 mmol), and the mixture was refluxed for 25 min (TLC). The reaction mixture was cooled to room temperature and evaporated in vacuo to give a yellow solid. The solid was dissolved in water (600 mL) and neutralized at 0 °C with concentrated HCl. The precipitate formed was removed by filtration, washed with a copious amount of water, and dried in vacuo to give the title compound **17** (16.7 g, 93%) as a pale yellow solid. Acid **17** was used in the subsequent step without further purification. An analytical sample of the product was obtained by crystallization from EtOH: mp 234.0−235.0 °C (EtOH). ^{1}H NMR (250 MHz, d_6-DMSO): δ 3.61 (s, 3H), 7.34 (t, J = 7.5 Hz, 1H), 7.72−7.90 (m, 5H), and 8.19 (∼d, J = 8.0 Hz, 1H). ^{13}C{^{1}H} NMR (63 MHz, d_6-DMSO): δ 31.83, 116.5, 121.6, 123.4, 125.2, 125.5, 125.8, 132.9, 133.5, 135.0, 137.1, 141.9, 149.5, 151.6, and 167.2. IR (KBr): υ_{max} 1742, 1696, 1518, 1468, 1339, and 1244 cm^{-1}. MS (ESI): *m*/*z* (rel intensity) 298 (100%, MH$^+$). HRMS calcd for $C_{15}H_{12}N_3O_4$ (MH$^+$) 298.0828, found 298.0838. Anal. Calcd for $C_{15}H_{11}N_3O_4$: C, 60.61; H, 3.73; N, 14.14. Found: C, 60.69; H, 3.65; N, 13.98.

2-(2-Aminophenyl)-1-methyl-1*H*-benzimidazole-4-carboxylic Acid (20). A suspension of benzimidazole **17** (16.1 g, 54.2 mmol) in MeOH (900 mL) was hydrogenated at normal pressure in the presence of Pd/C (10% w/w, 1.6 g) for 24 h (TLC). The resulting mixture was passed through a thin pad of Celite, and the filtrate was concentrated in vacuo to give the title compound **20** (14.4 g, 100%) as a yellow solid that could be used in the subsequent step without further purification. An analytical sample of the product was obtained by crystallization from EtOH: mp 214.0−215.0 °C (EtOH). ^{1}H NMR (250 MHz, d_6-DMSO): δ 3.69 (s, 3H), 5.77 (br s, 2H), 6.58 (∼t, J = 8.0 Hz, 1H), 6.75 (d, J = 8.0 Hz, 1H), 7.12 (dt, J = 7.5, 1.5 Hz, 1H), 7.25 (dd, J = 7.5, 1.5 Hz, 1H), 7.29 (t, J = 8.0 Hz, 1H), 7.72 (∼d, J = 7.5 Hz, 1H), and 7.77 (d, J = 8.0 Hz, 1H). ^{13}C{^{1}H} NMR (63 MHz, d_6-DMSO): δ 32.70, 112.2, 116.3, 116.4, 116.7, 120.3, 122.9, 125.0, 131.5, 132.0, 137.3, 142.0, 148.9, 154.6, and 167.3. IR (KBr): υ_{max} 1729, 1614, 1485, 1427, and 1385 cm^{-1}. MS (ESI): *m*/*z* (rel intensity) 268 (100%, MH$^+$). HRMS calcd for $C_{15}H_{14}N_3O_2$ (MH$^+$) 268.1086, found 268.1083. Anal. Calcd for $C_{15}H_{13}N_3O_2$: C, 67.40; H, 4.90; N, 15.72. Found: C, 67.12; H, 4.86; N, 15.66.

Cyclic Amide (5). To a suspension of amino acid **20** (2.75 g, 10.3 mmol) in CH_2Cl_2 (450 mL) was added NMM (2.5 mL, 23 mmol), followed by BOP (5.00 g, 11.3 mmol). The reaction mixture was stirred at room temperature for 6 days and washed with saturated $NaHCO_3$. The organic layer was dried ($MgSO_4$) and evaporated in vacuo to give a yellow solid. Purification by flash chromatography (silica gel, CH_2Cl_2 → EtOAc) gave the title compound **5** (1.17 g, 46%) as a white solid: R_f = 0.60 (EtOAc); mp > 260 °C (EtOAc). ^{1}H NMR (250 MHz, $CDCl_3$): δ 3.87 (s, 3H), 7.32−7.47 (m, 3H), 7.55−7.63 (m, 2H), 8.13 (d, J = 8.0 Hz, 1H), 8.18 (d, J = 7.5 Hz, 1H), and 12.1 (s, 1H). ^{13}C{^{1}H} NMR (101 MHz, $CDCl_3$): δ 32.11, 113.8, 122.0, 122.9, 123.0, 124.7, 124.8, 128.0, 130.1, 130.8, 136.3, 137.1, 140.2, 152.0, and 164.1. IR (KBr): υ_{max} 1665, 1533, 1516, 1481, 1434, 1380, and 1303 cm^{-1}. MS (ESI): *m*/*z* (rel intensity) 499 (100%, MH$^+$). HRMS calcd for $C_{30}H_{23}N_6O_2$ (MH$^+$) 499.1882, found 499.1865. Anal. Calcd for $C_{30}H_{22}N_6O_2$: C, 72.28; H, 4.45; N, 16.86. Found: C, 72.02; H, 4.39; N, 16.76. Single crystals of the cyclic amide **5** were grown by slow evaporation of a CH_2Cl_2/EtOAc solution, and its structure was unequivocally confirmed by single-crystal X-ray analysis. For crystallographic data, see Supporting Information.

Ni(II) Complex (25). To a suspension of cyclic amide **5** (809 mg, 1.62 mmol) in MeOH (70 mL) was added $Ni(OAc)_2 \cdot 4H_2O$ (425 mg, 1.70 mmol), and the mixture was refluxed for 90 min (TLC) to give an orange suspension. After being cooled to room temperature, the suspension was separated by filtration. The collected solid was washed with cold MeOH (30 mL) and dried to give the title compound **25** (875 mg, 97%) as a deep-orange solid: R_f = 0.45 (MeOH); mp > 260 °C (MeOH). ^{1}H NMR (250 MHz, d_4-MeOH + $CDCl_3$): δ 4.14 (s, 3H), 7.20−7.30 (m, 1H), 7.37−7.54 (m, 3H), 7.60−7.72 (m, 2H), and 7.99 (d, J = 7.5 Hz, 1H). ^{13}C{^{1}H} NMR (101 MHz, d_4-MeOH + $CDCl_3$): δ 34.73, 115.5, 122.3, 125.2, 125.8, 126.2, 126.6, 129.1, 132.5, 132.6, 137.4, 138.3, 149.4, 151.9, and 169.1. IR (KBr): υ_{max} 1606, 1562, 1526, 1485, 1437, 1325, and 1292 cm^{-1}. MS (ESI): *m*/*z* (rel intensity) 499 (10%, MH$^+$) and 499 (100). HRMS calcd for $C_{30}H_{21}N_6NiO_2$ (MH$^+$) 555.1079, found 555.1090. Anal. Calcd for $C_{30}H_{21.5}N_6NiO_{2.75}$ (M·0.75H_2O): C, 63.36; H, 3.81; N, 15.14. Found: C, 63.28; H, 3.89; N, 14.81. Single crystals of complex **25** were grown by slow evaporation of a CH_2Cl_2/MeOH solution, and its structure was unequivocally confirmed by single-crystal X-ray analysis. For crystallographic data, see Supporting Information. Ni(II) complex **25** was optically resolved by analytical CSP HPLC (Figure S1).

1,6-Bis(3-hydroxymethylphenoxy)hexane (34). To a solution of phenol **31** (15.0 g, 121 mmol) in EtOH (180 mL) was added 10 M NaOH (12.1 mL, 121 mmol), followed by 1,6-dibromohexane (14.8 g, 60.4 mmol). The reaction mixture was refluxed for 19 h, cooled to room temperature, and diluted with water (300 mL). The brown mixture was subsequently extracted with CH_2Cl_2, and the combined extracts were dried ($MgSO_4$) and concentrated in vacuo to give an off-white solid. Purification by flash chromatography (CH_2Cl_2 → CH_2Cl_2/Me_2CO, 4/1) gave the title compound **34** (12.9 g, 65%) as a slightly pink solid: R_f = 0.65 (EtOAc/CH_2Cl_2, 1/1); mp 93.0−94.0 °C (Me_2CO/petroleum ether). ^{1}H NMR (250 MHz, d_4-MeOH): δ 1.39−1.45 (m, 2H), 1.65−1.70 (m, 2H), 3.85 (t, J = 6.5 Hz, 2H), 4.44 (s, 2H), 6.67 (∼dd, J = 8.0, 2.5 Hz, 1H), 6.75−6.79 (m, 2H), and 7.09 (t, J = 8.0 Hz, 1H). ^{13}C{^{1}H} NMR (63 MHz, d_4-MeOH): δ 25.99, 29.38, 64.16, 67.84, 113.0, 113.4, 119.1, 129.4, 143.3, and 159.7. IR ($CHCl_3$): υ_{max} 2943, 2873, 1601, 1585, 1488, 1449, and 1264 cm^{-1}. MS (ESI): *m*/*z* (rel intensity) 353 (100%, MNa$^+$) and 313 (20). HRMS calcd for $C_{20}H_{26}NaO_4$ (MNa$^+$) 353.1729, found 353.1742. Anal. Calcd for $C_{20}H_{26}O_4$: C, 72.70; H, 7.93. Found: C, 72.61; H, 8.00.

1,6-Bis(3-bromomethylphenoxy)hexane (39). To a suspension of diol **34** (12.9 g, 39.0 mmol) in CH_2Cl_2 (400 mL) was added PBr_3 (4.8 mL, 51 mmol) at 0 °C, and the resulting clear solution was stirred at room temperature for 14 h. The reaction mixture was quenched with saturated $NaHCO_3$ (50 mL) and stirred at room temperature for an additional 30 min. The resulting white suspension was extracted with CH_2Cl_2, and the combined extracts were dried ($MgSO_4$) and evaporated in vacuo to give a white solid. Purification by flash chromatography (CH_2Cl_2/petroleum ether, 1/1) gave the title compound **39** (15.0 g, 84%) as a white solid: R_f = 0.80 (CH_2Cl_2/petroleum ether, 1/1); mp 87.0−88.0 °C (EtOAc/petroleum ether). ^{1}H NMR (250 MHz, $CDCl_3$): δ 1.44−1.49 (m, 2H), 1.70−1.76 (m, 2H), 3.89 (t, J = 6.5 Hz, 2H), 4.37 (s, 2H), 6.75 (ddd, J = 8.0, 2.0, 1.0 Hz, 1H), 6.83−6.89 (m, 2H), and 7.15 (t, J = 8.0 Hz, 1H). ^{13}C{^{1}H} NMR (63 MHz, $CDCl_3$): δ 26.34, 29.65, 34.07, 68.30, 115.1, 115.6, 121.6, 130.2, 139.6, and 159.8. IR ($CHCl_3$): υ_{max} 2944, 2871, 1600, 1585, 1489, 1446, and 1266 cm^{-1}. MS (ESI): *m*/*z* (rel intensity) 481 [50%, MNa$^+$ (^{81}Br/^{81}Br)], 479 [100%, MNa$^+$ (^{79}Br/^{81}Br)], and 477 [50%, MNa$^+$ (^{79}Br/^{79}Br)]. HRMS calcd for $C_{20}H_{24}(^{79}Br)_2NaO_2$ (MNa$^+$) 477.0041, found 477.0027. Anal. Calcd for $C_{20}H_{24}Br_2O_2$: C, 52.65; H, 5.30; Br, 35.03. Found: C, 52.87; H, 5.25; Br, 35.05.

1,6-Bis{3-[4-ethoxycarbonyl-2-(2-nitrophenyl)-benzimidazol-1-ylmethyl]phenoxy}hexane (43). To a solution of benzimidazole **11** (7.00 g, 22.5 mmol) in THF (100 mL) was added NaH (60% w/w dispersion in mineral oil, 990 mg, 25 mmol) at 0 °C. After 30 min, the reaction mixture was warmed to room temperature and stirred for an additional 40 min. The resulting brown solution was recooled to 0 °C and treated with dibromide **39** (5.13 g, 11.3 mmol). After 16 h at room temperature, the reaction mixture was quenched with water (10 mL), the volatiles were removed in vacuo, and the residue was partitioned between CH_2Cl_2 and water. The phases were separated, and the extraction was completed with additional portions of CH_2Cl_2. The combined organic extracts were dried ($MgSO_4$) and evaporated in vacuo

to give a yellow solid. Purification by flash chromatography (silica gel, $CH_2Cl_2 \rightarrow$ EtOAc) gave the title compound **43** (8.83 g, 86%) as a pale yellow solid: $R_f = 0.35$ (EtOAc); mp 179.0−181.0 °C (EtOAc). ^{1}H NMR (250 MHz, CD_2Cl_2): δ 1.30 (t, $J = 7.0$ Hz, 3H), 1.25−1.42 (m, 2H), 1.52−1.62 (m, 2H), 3.73 (t, $J = 6.5$ Hz, 2H), 4.31 (q, $J = 7.0$ Hz, 2H), 5.13 (s, 2H), 6.45 (d, $J = 1.5$ Hz, 1H), 6.50 (d, $J = 8.0$ Hz, 1H), 6.67 (dd, $J = 8.0$, 2.0 Hz, 1H), 7.06 (t, $J = 8.0$ Hz, 1H), 7.19 (t, $J = 7.5$ Hz, 1H), 7.37 (dd, $J = 8.0$, 1.0 Hz, 1H), 7.43−7.50 (m, 1H), 7.58−7.65 (m, 2H), 7.83 (dd, $J = 7.5$, 1.0 Hz, 1H), and 8.07−8.14 (m, 1H). ^{13}C{^{1}H} NMR (101 MHz, CD_2Cl_2): δ 14.98, 26.49, 29.82, 49.21, 61.59, 68.64, 113.6, 114.7, 115.8, 119.4, 123.1, 123.2, 125.7, 125.9, 126.6, 130.7, 132.1, 133.5, 134.3, 137.1, 137.7, 142.8, 149.6, 152.2, 160.4, and 166.4. IR ($CHCl_3$): υ_{max} 1716, 1604, 1534, 1453, 1429, 1346, and 1282 cm^{-1}. MS (ESI): *m*/*z* (rel intensity) 939 (20%, MNa^+) and 917 (100). HRMS calcd for $C_{52}H_{49}N_6O_{10}$ (MH^+) 917.3510, found 917.3497. Anal. Calcd for $C_{52}H_{48}N_6O_{10}$: C, 68.11; H, 5.28; N, 9.16. Found: C, 68.05; H, 5.40; N, 9.07.

1,6-Bis{3-[2-(2-aminophenyl)-4-ethoxycarbonylbenzimidazol-1-ylmethyl]phenoxy}hexane (47). To a suspension of benzimidazole **43** (8.83 g, 9.63 mmol) in anhydrous EtOH (200 mL) was added $SnCl_2$ (18.3 g, 96.3 mmol), and the mixture was refluxed for 50 min to give a yellow solution. The reaction mixture was cooled in an ice bath, diluted with CH_2Cl_2 (300 mL), and made basic by addition of saturated $NaHCO_3$. After 30 min at room temperature, the resulting white suspension was filtered through a pad of Celite. The phases were separated, and the extraction was completed with additional portions of CH_2Cl_2. The combined organic extracts were dried ($MgSO_4$) and evaporated in vacuo to give a yellow solid. Purification by flash chromatography (silica gel, $CH_2Cl_2 \rightarrow$ EtOAc) gave the title compound **47** (8.09 g, 98%) as a pale yellow solid: $R_f = 0.75$ (EtOAc). ^{1}H NMR (250 MHz, $CDCl_3$): δ 1.20−1.30 (m, 2H), 1.33 (t, $J = 7.0$ Hz, 3H), 1.50−1.60 (m, 2H), 3.70 (t, $J = 6.5$ Hz, 2H), 4.37 (q, $J = 7.0$ Hz, 2H), 5.27 (s, 2H), 5.47 (br s, 2H), 6.41−6.55 (m, 3H), 6.65−6.69 (m, 2H), 6.99−7.14 (m, 4H), 7.22 (dd, $J = 8.0$, 1.0 Hz, 1H), and 7.84 (dd, $J = 7.5$, 1.0 Hz, 1H). ^{13}C{^{1}H} NMR (63 MHz, $CDCl_3$): δ 14.93, 26.21, 29.49, 49.14, 61.28, 68.21, 112.6, 112.7, 114.2, 115.3, 117.3 (2 × C), 118.5, 121.6, 122.5, 125.7, 129.9, 130.6, 131.1, 131.5, 137.0, 138.2, 142.2, 148.6, 154.9, 160.2, and 166.8. IR ($CHCl_3$): υ_{max} 1707, 1617, 1602, 1488, 1428, 1290, 1265, and 1251 cm^{-1}. MS (ESI): *m*/*z* (rel intensity) 870 (50%, MNa^+) and 857 (100). HRMS calcd for $C_{52}H_{53}N_6O_6$ (MH^+) 857.4026, found 857.4015.

1,6-Bis{3-[2-(2-aminophenyl)-4-hydroxycarbonylbenzimidazol-1-ylmethyl]phenoxy}hexane (51). To a solution of ester **47** (8.09 g, 9.44 mmol) in THF (230 mL) was added 1 M LiOH (58 mL, 58 mmol), and the mixture was stirred at room temperature for 20 h. The reaction mixture was evaporated in vacuo, and the residue was suspended in water (300 mL) and brought to pH 5 by addition of 1 M HCl. The resulting suspension was stirred at room temperature for 2 h and filtered. The precipitate was collected, washed with a copious amount of water, and dried in vacuo to give the title compound **51** (6.95 g, 92%) as a pale yellow solid that could be used in the subsequent step without further purification. Amino acid **51**. ^{1}H NMR (400 MHz, d_6-DMSO): δ 1.29−1.36 (m, 2H), 1.54−1.67 (m, 2H), 3.83 (t, $J = 6.5$ Hz, 2H), 5.49 (s, 2H), 5.89 (br s, 2H), 6.55−6.62 (m, 2H), 6.64 (t, $J = 7.0$ Hz, 1H), 6.77 (dd, $J = 7.5$, 2.0 Hz, 1H), 6.89 (d, $J = 8.0$ Hz, 1H), 7.15 (t, $J = 7.0$ Hz, 1H), 7.23 (dt, $J = 7.0$, 1.5 Hz, 1H), 7.28 (dd, $J = 7.5$, 1.0 Hz, 1H), 7.35 (t, $J = 8.0$ Hz, 1H), 7.76 (d, $J = 8.0$ Hz, 1H), and 7.83 (d, $J = 7.5$ Hz, 1H). ^{13}C{^{1}H} NMR (101 MHz, d_6-DMSO): δ 25.57, 28.84, 48.11, 67.60, 112.0, 113.0, 114.1, 116.0, 116.3 (2 × C?), 118.8, 120.3, 122.7, 124.7, 130.2, 130.5, 131.6, 136.0, 138.3, 141.8, 148.3, 154.1, 159.2, and 166.8. IR (KBr): υ_{max} 1740, 1610, 1488, 1433, 1388, and 1260 cm^{-1}. MS (ESI): *m*/*z* (rel intensity) 801 (100%, MH^+). HRMS calcd for $C_{48}H_{44}N_6NaO_6$ (MNa^+) 823.3220, found 823.3189.

Monomer (55) and Dimer (59). To a solution of amino acid **51** (3.00 g, 3.75 mmol) in CH_2Cl_2 (400 mL) was added NMM (1.8 mL, 16 mmol), followed by BOP (3.64 g, 8.24 mmol). The resulting yellow solution was stirred at room temperature for 10 days and quenched with saturated $NaHCO_3$ (100 mL). After 1 h at room temperature, the phases were separated, and the extraction was completed with additional portions of CH_2Cl_2. The combined organic extracts were dried ($MgSO_4$) and evaporated in vacuo to give a brown thick oil. Purification by flash chromatography (silica gel, $CH_2Cl_2 \rightarrow CH_2Cl_2$/MeOH, 20/1) gave monomer **55** (288 mg, 10%) and dimer **59** (363 mg, 13%) as white solids. Monomer **55**: $R_f = 0.65$ (CH_2Cl_2/EtOAc, 5/1); mp > 260 °C (EtOAc). ^{1}H NMR (400 MHz, $CDCl_3$): δ 0.33−0.38 (m, 2H), 0.59−0.64 (m, 2H), 3.41 (t, $J = 6.0$ Hz, 2H), 5.30 and 5.78 (ABq, $J = 16.0$ Hz, 2H), 5.71 (s, 1H), 6.62 (dd, $J = 8.0$, 2.0 Hz, 1H), 6.79 (d, $J = 7.5$ Hz, 1H), 7.14 (t, $J = 8.0$ Hz, 1H), 7.27 (t, $J = 8.0$ Hz, 1H), 7.59 (ddd, $J = 9.0$, 9.0, 1.5 Hz, 1H), 8.13 (dd, $J = 7.5$, 1.0 Hz, 1H), 8.14 (d, $J = 7.5$ Hz, 1H), and 12.2 (s, 1H). ^{13}C{^{1}H} NMR (63 MHz, $CDCl_3$): δ 25.03, 27.97, 49.48, 67.20, 110.8, 115.7, 117.1, 119.2, 122.3, 123.3, 123.5, 125.2, 125.4, 128.2, 130.1, 130.4, 131.4, 135.5, 136.7, 137.9, 140.9, 153.0, 159.6, and 163.9. IR (KBr): υ_{max} 1673, 1607, 1583, 1534, 1478, 1386, 1302, and 1248 cm^{-1}. MS (ESI): *m*/*z* (rel intensity) 787 (100%, MNa^+) and 765 (15). HRMS calcd for $C_{48}H_{40}N_6NaO_4$ (MNa^+) 787.3009, found 787.2993. Anal. Calcd for $C_{48}H_{40}N_6O_4$: C, 75.37; H, 5.27; N, 10.99. Found: C, 75.08; H, 5.23; N, 10.93. Monomer **55** was optically resolved by analytical CSP HPLC (Figure S7). Dimer **59**: $R_f = 0.40$ (CH_2Cl_2/EtOAc, 5/1). ^{1}H NMR (400 MHz, d_6-DMSO): δ 0.95 (br s, 4H), 1.25 (br s, 4H), 3.47−3.54 (m, 4H), 5.50−5.60 (m, 4H), 6.23 (s, 1H), 6.27 (s, 1H), 6.57 (d, $J = 7.5$ Hz, 1H), 6.61 (d, $J = 7.5$ Hz, 1H), 6.65 (d, $J = 8.0$ Hz, 2H), 7.04 (t, $J = 7.5$ Hz, 1H), 7.06 (t, $J = 7.5$ Hz, 1H), 7.31 (t, $J = 8.0$ Hz, 1H), 7.35 (t, $J = 8.0$ Hz, 1H), 7.40 (t, $J = 7.5$ Hz, 2H), 7.63 (t, $J = 7.5$ Hz, 2H), 7.69 (d, $J = 8.0$ Hz, 1H), 7.73 (d, $J = 8.0$ Hz, 1H), 7.75 (d, $J = 8.0$ Hz, 2H), 7.95 (d, $J = 7.5$ Hz, 1H), 8.00 (dd, $J = 8.0$, 3.0 Hz, 2H), 11.90 (s, 1H), and 11.91 (s, 1H). ^{13}C{^{1}H} NMR (63 MHz, $CDCl_3$): δ 25.27, 28.52, 48.15, 67.24, 67.28, 112.1, 112.3, 114.1, 116.3, 118.8, 118.9, 122.1, 122.2, 122.5, 123.2, 124.4, 125.7, 127.5, 130.2, 130.5, 131.1, 131.2, 135.6 (2 × C), 136.8, 137.7, 139.8, 152.1 (2 × C), 159.1 (2 × C), and 162.8. IR (KBr): υ_{max} 1672, 1607, 1583, 1533, 1487, 1427, 1385, 1302, and 1247 cm^{-1}. MS (ESI): *m*/*z* (rel intensity) 1530 (100%, MH^+). HRMS calcd for $C_{96}H_{80}N_{12}NaO_8$ (MNa^+) 1551.6120, found 1551.6127. Anal. Calcd for $C_{96}H_{80}N_{12}O_8$: C, 75.37; H, 5.27; N, 10.99 or for $C_{96}H_{81}N_{12}O_{8.5}$ ($M{\cdot}0.5H_2O$): C, 74.93; H, 5.31; N, 10.92. Found: C, 74.95; H, 5.37; N, 10.96.

Optical Resolution of the Strapped Cyclic Amide (55). The enantiomers of the strapped cyclic amide **55** were separated on a semipreparative scale by CSP HPLC (Chiralcel OD column, 1.0 cm × 25 cm; 2-propanol/hexanes, 40/60; 4 mL min^{-1}, 40 °C). UV detection was performed at 254 nm. Injections of ∼0.5 mg of the racemate in 50 μL of CH_2Cl_2 were made every 30 min. The fast-eluting enantiomer was collected between 11.8 and 16.1 min, and the slow-eluting enantiomer was collected between 19.0 and 26.5 min. The collected products were enantiomerically pure (ee > 99.9% and 99.5%, respectively) by analytical CSP HPLC and were used in the subsequent racemization studies (see Table 1).

Ni(II) Complex (62). To a suspension of strapped cyclic amide **54** (59 mg, 80 μmol) in CH_2Cl_2/MeOH (1/1, v/v, 5 mL) was added $Ni(OAc)_2{\cdot}4H_2O$ (22 mg, 88 μmol), and the mixture was refluxed for 15 h (TLC) to give a deep-orange suspension. After being cooled to room temperature, the suspension was concentrated to ∼2 mL and filtered off. The collected solid was washed with cold MeOH (2 mL) and dried to give the title compound **62** (60 mg, 94%) as a deep-orange solid: $R_f = 0.70$ (MeOH). ^{1}H NMR (250 MHz, $CDCl_3$): δ 0.72−0.94 (m, 1H), 1.43−1.65 (m, 1H), 3.25−3.42 (m, 1H), 3.70−3.88 (m, 1H), 5.17 (s, 1H), 5.56 and 6.11 (ABq, $J = 16$ Hz, 2H), 6.64 (dd, $J = 8.0$, 2.0 Hz, 1H), 6.88 (d, $J = 7.5$ Hz, 1H), 7.12−7.35 (m, 4H), 7.46 (dt, $J = 7.5$, 1.5 Hz, 1H), 7.57 (dd, $J = 7.5$, 1.0 Hz, 1H), 7.63 (d, $J = 8.0$ Hz, 1H), and 8.08 (d, $J = 7.5$ Hz, 1H). ^{13}C{^{1}H} NMR (101 MHz, $CDCl_3$): δ 26.10, 50.95, 66.71, 107.7, 115.3, 118.2, 118.3, 120.5, 123.9, 125.1, 125.2, 125.8, 127.5, 130.3, 131.8, 132.2, 135.1, 136.4, 138.0,

149.3, 154.7, 158.9, and 165.9. IR (KBr): υ_{max} 1604, 1576, 1480, 1433,1414, 1320, 1292, and 1262 cm^{-1}. MS (ESI): *m*/*z* (rel intensity) 793 (25%, M^+) and 737 (100). HRMS calcd for $C_{46}H_{34}N_6NaNiO_4$ (MNa^+) 815.1893, found 815.1887. Crystals suitable for X-ray diffraction analysis were grown by slow evaporation of a CH_2Cl_2/MeOH solution. For crystallographic data, see Supporting Information. The Ni(II) complex **62** was optically resolved by analytical CSP HPLC (Figure S9).

Acknowledgment. This work was supported by the National Science Foundation (CAREER Award No. 9984071).

Supporting Information Available: Synthetic procedures for the compounds not described in the Experimental Section; selected CSP HPLC profiles; solutions and refinement, atomic coordinates, bond lengths and angles, anisotropic thermal parameters, and CIF files for **5**, **25**, **26**, and **62**; copies of ^1H and ^{13}C NMR spectra for all new compounds (PDF). This material is available free of charge via the Internet at http://pubs.acs.org.

JA030196D